

**REPUBLIC OF TURKEY
AYDIN ADNAN MENDERES UNIVERSITY
GRADUATE SCHOOL OF NATURAL AND APPLIED SCIENCES
MECHANICAL ENGINEERING
2019-M.Sc.-89**



**THERMAL PERFORMANCE ANALYSIS OF
FLAT-PLATE SOLAR COLLECTOR USING
NANOFLUIDS**

Zafer Yavuz AKSÖZ

Supervisor:

Prof.Dr. İsmail BÖĞREKÇİ

AYDIN

REPUBLIC OF TURKEY
AYDIN ADNAN MENDERES UNIVERSITY
GRADUATE SCHOOL OF NATURAL AND APPLIED SCIENCES

The thesis with the title of “Thermal Performance Analysis of Flat-Plate Solar Collector Using Nanofluids” prepared by the Zafer Yavuz Aksöz, Master Student at the Mechanical Engineering Program at the Department of Mechanical Engineering was accepted by the jury members whose names and titles presented below as a result of thesis defence on 11.06.2019.

	Title, Name Surname	Institution	Signature
President :	
Member :	
Member :	

This Master Thesis accepted by the jury members is endorsed by the decision of the Institute Board Members with <.....> Serial Number and <.....> date.

Prof. Dr. Gönül AYDIN
Institute Director

REPUBLIC OF TURKEY
AYDIN ADNAN MENDERES UNIVERSITY
GRADUATE SCHOOL OF NATURAL AND APPLIED SCIENCES

I hereby declare that all information and results reported in this thesis have been obtained by my part as a result of truthful experiments and observations carried out by the scientific methods, and that I referenced appropriately and completely all data, thought, result information which do not belong my part within this study by virtue of scientific ethical codes.

.../.../2019

Signature

Zafer Yavuz Aksöz

ÖZET

Nanoakışkanlı Düzlemsel Güneş Kollektörünün Isıl Performans Analizi

Zafer Yavuz AKSÖZ

Yüksek Lisans Tezi, Makine Mühendisliği ABD

Tez Danışmanı: Prof.Dr. İsmail BÖĞREKÇİ

2019, 99 sayfa

Son yıllarda yenilenebilir enerji kaynaklarına ilgi giderek artmaktadır. Güneş enerjisi bu kaynaklar arasında dünya üzerinde hemen hemen her yerde mevcut olan tek enerji kaynağı ve sınırsız olduğundan değerlendirilmesi gerekmektedir. Bu çalışmada literatürdeki termal güneş enerji sistemleri ve nanoakışkanların hazırlanışı, ısı transferi, akış teorileri ve sonuçları incelenmiştir. Test simülasyonu için düzlemsel güneş kolektörleri matematiksel olarak modellenip programı yazılmıştır. Tasarlanan bu kolektörün performansı %1 ve %5 lik karıştırma oranları ile hazırlanmış Al_2O_3 ve Cu nanoakışkanları kullanılarak simülasyon programında test edilmiştir. Test sonuçlarına göre Cu başta olmak üzere kullanılan nanoakışkanlar kolektör verimini artırmıştır. Böylece sıvıyı ısıtmak için gerekli kolektörün masrafı azaltılmıştır.

Anahtar Kelimeler: Al_2O_3 , Cu, düzlemsel, güneş kolektörü, ısıl verim, nano akışkan

ABSTRACT

THERMAL PERFORMANCE ANALYSIS OF FLAT PLATE SOLAR COLLECTOR USING NANOFLUIDS

Zafer Yavuz AKSÖZ

Msc. Thesis, Department of Mechanical Engineering

Supervisor: Prof.Dr. İsmail Bögrekçi

2019, 99 pages

In recent years, there has been an increasing interest in renewable energy resources. Since solar energy is the only resource available at almost any location around the world and limitless, it should be utilized. In this study, the literature related to solar thermal energy systems and synthesis, theoretical background of nanofluids reviewed. A detailed mathematical model designed and programmed for simulating flat-plate solar collector. A flat-plate collector, which includes 1% and 5% volume concentration of two different nanofluids: Cu and Al_2O_3 , designed and tested in the simulation. According to the obtained results, nanofluids in particular Cu nanofluid increased the efficiency of the collector. Therefore, the cost for heating the liquid was decreased.

Key Words: Al_2O_3 , Cu, flat-plate, thermal efficiency, nanofluids, solar collector

ACKNOWLEDGEMENTS

During the writing of this thesis I have received a great deal of support and assistance. I would like to thank my supervisor, Prof.Dr. İsmail Böğrekcı.

I would like to acknowledge my colleagues and friends who were always willing to help me.

In addition, I would like to thank my parents for their patience and support over the course of my research.

Zafer Yavuz AKSÖZ

TABLE OF CONTENTS

ÖZET.....	vii
ABSTRACT.....	ix
ACKNOWLEDGEMENTS.....	xi
1.INTRODUCTION.....	1
1.1.Flat-Plate Solar Collectors in History.....	5
1.2.Solar Energy Use in History.....	6
1.3.Solar Thermal Systems.....	8
1.3.1.Flat-Plate Solar Collector.....	9
1.3.2.Evacuated Tube Solar Collectors.....	12
1.3.2.1.Heat Pipe Evacuated Tube Solar Collector.....	12
1.3.2.2.Direct Flow ETC.....	13
1.3.2.3.Thermal Tube Collector (TTC).....	13
1.3.3.Solar Air Collectors.....	14
1.3.4.Concentration Solar Collectors.....	15
1.3.4.1.Parabolic Trough CSC.....	15
1.4.Solar Energy.....	16
1.4.1.Solar Radiation.....	16
1.4.2.The Source of Solar Energy.....	16
1.4.2.1.The Solar Constant.....	19
1.4.2.2.Fluctuation of Extra-Terrestrial Radiation.....	21

1.4.2.3.Types of Solar radiation	22
1.4.2.4.Angles and Directions of Solar Radiation	23
1.4.2.5.Solar Time	24
2.LITERATURE REVIEW	26
2.1.Review of Nanofluid	26
2.1.1.Synthesis of Nanofluids.....	27
2.1.1.1.Two Steps Method.....	27
2.1.1.2.One Step Method.....	29
2.1.2.Types of Nanofluids	29
2.1.3.Thermal Conductivity Measurement Methods	30
2.1.3.1.Transient hot wire method.....	30
2.1.3.2.Thermal constants analyser methods	31
2.1.3.3.Steady-State Parallel Plate Technique.....	32
2.1.4.The Effects on the thermal conductivity change of nanofluid.....	33
2.1.4.1.Particle Size	33
2.1.4.2.Particle Shape	34
2.1.4.3.Particle Material	35
2.1.4.4.Volume Concentration.....	35
2.1.4.5.Temperature.....	36
3.MATERIALS AND METHODS	36
3.1.Heat Transfer Theory	36

3.1.1.Heat Transfer by Conduction	38
3.1.1.1.Thermal Conductivity	39
3.1.2.Heat Transfer by Convection	40
3.1.3.Heat Transfer by Radiation	40
3.1.4.Thermophysical Features of Nanofluids	41
3.2.Mathematical Model	44
3.3.Heat Losses	46
3.3.1.Overall Heat Loss Coefficient.....	46
3.3.2.Top Heat Loss Coefficient	48
3.4.Heat transfer Coefficient of the Working Fluid	53
3.5.Useful Heat Gain and Thermal Efficiency	59
3.6.Modelling Simulation.....	61
3.6.1.Model of the Top Heat Loss Coefficient.....	63
3.6.2.Convection Heat Transfer of the fluid.....	65
3.6.3.Efficiency Modelling.....	65
3.7.Experiment Materials	66
4.RESULTS AND DISCUSSION	68
4.1.Top heat losses	68
4.2.Fluid Inlet and Outlet Temperatures	69
4.3.Useful Heat Gain.....	72
4.4.Efficiency	74

5.CONCLUSIONS	78
REFERENCES	80
APPENDIXES.....	84
Appendix 1. Function Library for Top Heat Loss Coefficient Calculation.....	84
Appendix 2. Collector Top Heat Loss Coefficient	86
Appendix 3. Function Library for Convection heat transfer Coefficient	90
Appendix 4. Heat Transfer Coefficient of the 1% Al ₂ O ₃ Nanofluid	91
Appendix 5. Function Library for Collector Efficiency Calculation.....	93
Appendix 6. Flat-plate Solar Collector Efficiency Calculation.....	95
Personel Information	99



LIST OF SYMBOLS

α	: Absorptance
β	: Slope
γ	: Surface azimuth angle, bond thickness
δ	: Declination, thickness (defined locally)
ϵ	: Emittance
η	: Efficiency of the collector
θ	: Angle (defined locally)
λ	: Wavelength
μ	: Dynamic viscosity
ν	: Kinematic viscosity
ρ	: Density
ρ_{nf}	: Density of the nanofluid
μ	: Dynamic viscosity
σ	: Stephan-Boltzmann Constant
τ	: Transmittance
ϕ	: Volumetric concentration, latitude, angle (defined locally)
ω	: Hour angle



LIST OF ABBREVIATIONS

A_c	: Collector area (m^2)
C_p	: Specific heat of the fluid (J/kg K)
W	: Tube spacing
D	: Tube diameter
F_R	: Heat removal factor
F'	: Collector efficiency factor
F''	: Collector flow factor
k	: Thermal conductivity
k_{eff}	: Effective thermal conductivity
FPSC	: Flat-plate solar collector
CSC	: Concentrated solar collector
ETC	: Evacuated tube solar collector
G_T	: Incident solar radiation (W/m^2 K)
\dot{m}	: Mass flow rate of fluid (kg/s)
Q_u	: Useful power of solar collector (W)
U_L	: Overall heat loss coefficient (W/m^2K)
V	: Velocity of the fluid (m/s)
S	: Absorbed solar radiation per unit area
T	: Temperature (defined locally)
EG	: Ethylene glycol

TEM : Transmission Electron Microscope



LIST OF FIGURES

Figure 1.1 Global Carbon dioxide emission.....	2
Figure 1.2 CO ₂ emissions of Turkey from 1900 to 2016 in Mt	2
Figure 1.3 Total final consumption by source in ktoe in the World.....	3
Figure 1.4 Total final consumption by source in Turkey between 1990 and 2016 ..	4
Figure 1.5 Cross sectional view of the common flat-plate solar collector	10
Figure 1.6 Heat Pipe ETC	12
Figure 1.7 Direct Flow ETC.....	13
Figure 1.8 Illustration of thermal tube solar collector.....	14
Figure 1.9 Solar air collector.....	14
Figure 1.10 Schematic of Parabolic Trough Concentrated Solar Collector	15
Figure 1.11 The structure of the Sun.....	18
Figure 1.12 Geometry of the solar constant	19
Figure 1.13 The total solar irradiance in the years between 1976 to 2017. The black vertical line shows the solar constant.....	20
Figure 1.14 Monthly Solar radiation over the year	21
Figure 1.15 Total Solar Radiation as the sum of beam, diffuse and reflected radiation.....	Hata! Yer işareti tanımlanmamış. 23
Figure 1.16 E values in minutes during the year	25
Figure 2.1 Preparation of nanofluid by two steps method	28
Figure 2.2 TEM image of Cu nanofluid prepared using one step method	29

Figure 2.3 Schematic drawing of common hot wire cell and the related electrical circuit.....	31
Figure 2.4 Diagram of the thermal constant analyser setup measurement.	32
Figure 2.5 A schematic diagram of steady-state parallel plate method.....	32
Figure 2.6 Effective thermal conductivity of the two different nanofluids including two different shapes SiC-26 and SiC-600 in DI-H ₂ O.....	34
Figure 3.1 Heat conduction from the element	38
Figure 3.2 Components of FPSC: (a) cross-sectional view (b) isometric view.....	45
Figure 3.3 Heat losses from flat-plate solar collector in cross sectional view.	46
Figure 3.4 Thermal resistance network of single cover flat-plate solar collector with respect to resistances between plates.....	49
Figure 3.5 A brief overview of the thermal resistance network	49
Figure 3.6 Tube and absorber plate dimensions	53
Figure 3.7 Energy balance in control volume of flow in pipe element	55
Figure 3.8 Energy balance of the control volume in the tube of the FPSC	55
Figure 3.9 Collector flow factor with dimensionless collector capacitance rate ...	59
Figure 3.10 Flowchart of top heat loss coefficient program.....	64
Figure 4.1 Top heat loss coefficient of the collector with absorber plate temperature	68
Figure 4.2 Collector outlet temperatures of Water, Al ₂ O ₃ 1% and Cu 1% with their inlet temperatures.	69
Figure 4.3 Collector outlet temperatures of Water, Al ₂ O ₃ 5% and Cu 5% with their inlet temperatures.	71

Figure 4.4 Useful heat gain of the collector with fluid inlet temperature using three different working fluids: Water, Al ₂ O ₃ 1% and Cu 1%.	72
Figure 4.5 Useful heat gain of the collector with fluid inlet temperature using three different working fluids: Water, Al ₂ O ₃ 5% and Cu 5%.	73
Figure 4.6 Efficiency of a common single glazed flat-plate solar collector.....	74
Figure 4.7 Efficiency of flat-plate collector using water with reduced temperature parameter.....	75
Figure 4.8 Efficiency of flat-plate collectors using Water, Al ₂ O ₃ 1% and Cu 1% with reduced temperature parameter.	76
Figure 4.9 Instantaneous efficiency of the flat-plate solar collector with water, 5% Al ₂ O ₃ and 5% Cu.....	77

LIST OF TABLES

Table 3.1 Collector parameters..... 62

Table 3.2 Thermal properties of nanofluids 67





LIST OF APPENDIXES

Appendix 1. Function Library for Top Heat Loss Coefficient Calculation	88
Appendix 2. Collector Top Heat Loss Coefficient	90
Appendix 3. Function Library for Convection heat transfer Coefficient	92
Appendix 4. Heat Transfer Coefficient of the 1% Al ₂ O ₃ Nanofluid	94
Appendix 5. Function Library for Collector Efficiency Calculation.....	95
Appendix 6. Flat-plate Solar Collector Efficiency Calculation.....	97



1. INTRODUCTION

Industrial revolution in the nineteenth century was the time when CO₂ emissions began to increase significantly. Carbon dioxide, methane, nitrous oxide etc. in gaseous phase are called greenhouse gaseous and they absorb more heat due to their higher specific heat capacities than the gases in the natural atmosphere therefore making the atmosphere denser and warmer. They also prevent some heat reflecting from ground to the space and therefore results in temperature enhancement of the atmosphere.

Temperature increment of the earth is called global warming. CO₂ gases are commonly believed to cause global warming as it is obvious from the human factor and usage of the fossil fuels in industries. Fossil fuels not only utilized in generating electricity in power plants but also used for powering vehicles, heating place, producing plastics and so on. This intense and continuous consumption of the fossil fuels and release of greenhouse gases affect the sustainability and health of the biological life directly or indirectly by changing environment such as melting ices, increasing temperature of locations which natural habitat is balanced and depends on it. Unfortunately, the world has been mostly aware of these hazardous effects; however, the precautions so far have been remained inadequate.

The problems mentioned above bring us to only one conclusion that more and better precautions are necessary to reduce CO₂ emissions by mainly utilizing renewable energy resources. For this reason, solar energy is a good alternative since it is a renewable energy resource and can be used for many purposes such as electricity production, water heating, space heating etc.

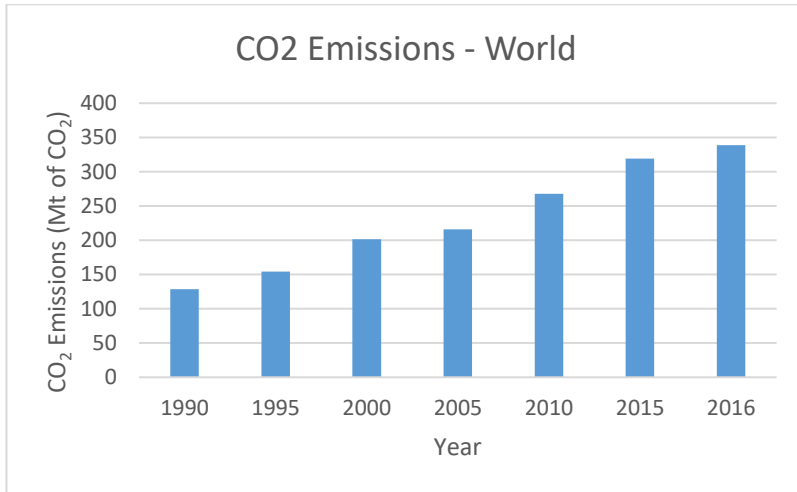


Figure 1.1 Global Carbon dioxide emission (IEA,2019)

From the Figure 1.1 Global Carbon dioxide emission (IEA,2019)it can be seen that carbon dioxide emission increased in the world during the 16 years.

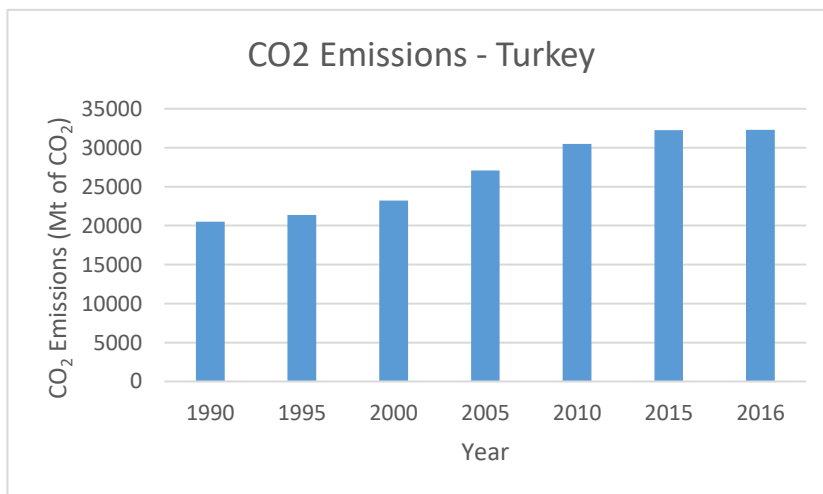


Figure 1.2 CO₂ emissions of Turkey from 1900 to 2016 in Mt (IEA,2019)

As can be seen from the Figure 1.2 CO₂ emissions of Turkey from 1900 to 2016 in Mt (IEA,2019) that CO₂ emission of Turkey over the 16 years increased. Comparing

the Figure 1.1 it is apparent that carbon dioxide emission increment over the last three years is greater than the global increment rate. In other words, many countries currently have lesser carbon dioxide emissions. Therefore, Turkey should utilize energy resources releasing less or zero carbon dioxide. Solar energy can save lots of energy produced by combusting fossil fuels.

The bar chart in Figure 1.3 demonstrates the total final consumption (TFC) by resources in the world in ktce from 1990 to 2016. Also, after 1990 crude oil has almost been not used. The majority of the resources belongs to the oil products as a fossil fuel for all years and it is not renewable and the main cause of CO₂ emissions. The usage of geothermal, solar, wind etc. energy resources have been increased since 2000. After 1996, the usage of combustible renewable energy resources such as biofuels and waste etc. have been increased slightly. Electricity consumption evened out at approximately the same level until 1995 but suddenly increased by the following the year of 2000 until 2015.

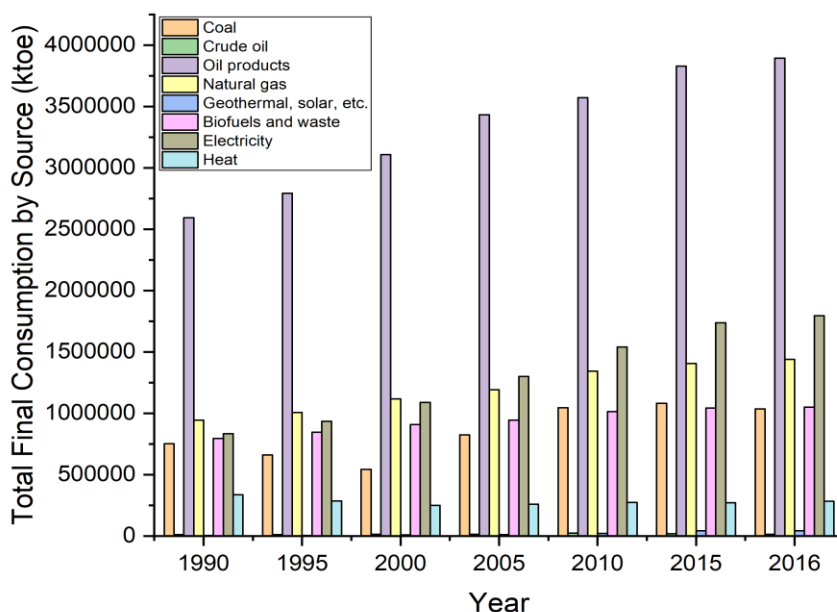


Figure 1.3 Total final consumption by source in ktce in the World(IEA,2019)

However, over the following year there was not a considerable increase in consumption of electricity. Heat, on the other hand, has been in use over the years and remained constant. Thus, heat and electricity as a resource are to be chiefly focused on.

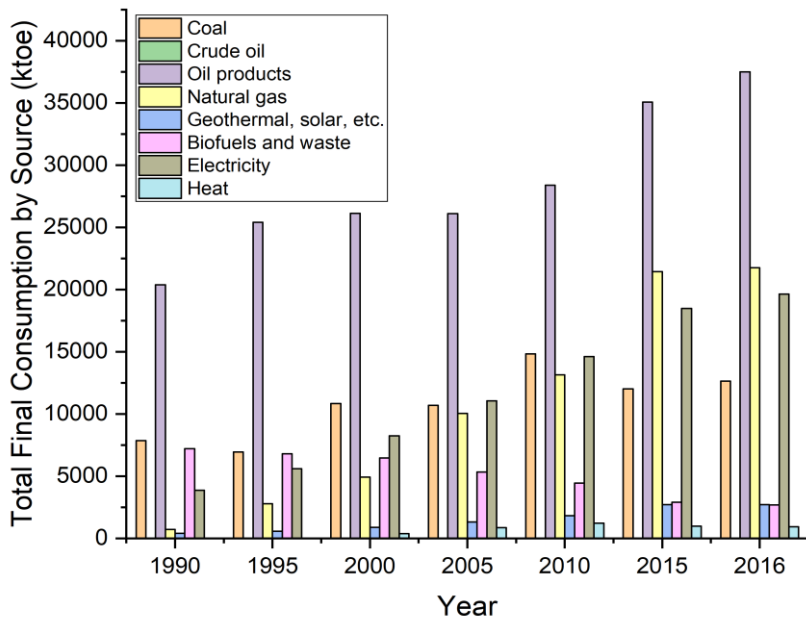


Figure 1.4 Total final consumption by source in Turkey between 1990 and 2016(IEA,2019)

The bar chart above shows the total final consumption by different resources in Turkey. From Figure 1.4 it can be seen that consumption of oil products for energy production has been increased tremendously in Turkey after 2010. Turkey needs energy production systems more than many countries. Natural gas consumption is gradually increasing over the years seen in graph. Coal, on the other hand, fluctuated over the years but the last two years saw no major change but over the years it has been in use. The amount of electricity consumption rose by a stable percentage every year. Forecasts show that electricity consumption and the fossil fuels used to

produce electricity will grow in the future. Thus, solar energy can be an alternative energy resource in order to use for many purposes such as producing electricity or heat.

1.1. Flat-Plate Solar Collectors in History

Flat-plate solar collectors are major type of solar water heating systems. It has cheap and simple structure, besides production and installation processes are very easy; therefore, it has been in use for more than half century.

The main applications of flat-plate solar collectors are for heating liquid, which is mostly chosen as water or water mixtures such as antifreeze & water mixture to prevent freezing in cold climate conditions. Although, water has been used as a working fluid in flat-plate solar collector for decades, novel liquids like nanofluids have been used to increase its performance. Common nanofluids and their properties will be introduced in later chapters of this thesis.

Flat-plate solar collectors which are used for water heating consists of some main parts: glass cover, absorber plate and insulation. An absorber plate includes pipes allowing liquid phase fluid inside while the collector working naturally or by force. These pipes can be seen as attached or integrated to absorber plate and this plate should has high thermal conductivity to be able to convert solar radiation into heat, which is absorbed by the working fluid. Thus, it is generally chosen as aluminium, copper or steel. Using these metallic materials is also give the absorber to resist high temperatures reaching 200 °C, which is the utmost flat-plate absorber temperature. Transparent cover is generally selected as glass to allow the solar rays pass to absorber as much as possible. The insulation attached to back and sides of the flat-plate solar collector keeps the heat inside.

This thesis seeks to examine the developments of Flat-plate solar collector together with nanofluids. To do so, the flat-plate solar collector mathematical model generated and a related experiment was conducted. In addition to mathematical

model, to determine top heat loss coefficient of FPSC, a program was written in Python 3.7 .

As the context of the study was mentioned above, the thesis will review the literature first and then will explain and compare the results, finally it will present the conclusions and suggest future research.

1.2. Solar Energy Use in History

Solar energy has been used for almost all the time. Not only people but also all the world use the solar energy from the beginning. The increasing interest of solar energy is promising in order to decrease the pollution of fossil fuels.

The source of solar energy is nuclear fusion in the Sun. The earth than exposed to this solar radiation almost every time apart from the periods like solar eclipse. Due to the structure of the world, the sun rays reach only the half of the world and not the same intensity at the same time. These differences create some challenges in using solar energy. Therefore, the solar rays cannot reach directly to the earth surface and always some of them are absorbed, reflected or they even never appear on the sky during the night. And it also depends on location of the surface that is considered. Together with location, the daytime period and the angles of the Sun over the year vary hence they affect the solar energy income and utilization significantly.

The earliest usage of solar energy can be seen in the history of Greek and Romans in which people built house entrance and windows looking to south. This allows sunlight to reach inside of the houses longer time periods of any day of a year. Thanks to these advances in solar energy utilization they benefited from it by heating or using as solar light.

Another usage of solar energy was to ignite materials that is easy to get fire like leaves by using magnifying glasses in 7th century B.C.

In 1941, first solar cells were produced and showed an alternative way to produce electricity to the world and therefore accepted as a beginning of a new renewable energy resource but solar cells were so expensive that they could not be afforded and were not able to compete the conventional power producing systems in 1950s. The first solar cells were manufactured only with an efficiency of 1%. However, after seeing the improvements in solar cells, it is understood that solar energy can be converted to electricity in an easy way. In addition, expensive cost of the first solar cells around 300 \$ in 1954 has been considerably decreased up to 20 \$ in 1970s. The decreasing trend of solar cells and PV panes have been continued until recently. Considering the great interest in solar energy, this trend seems to increase in the future, because the manufacturers today are in a contest all over the world.

The first PV panel usage on satellites was dated back to 1958 with Vanguard 1. Later, In 1960s the satellites of USA and Soviet's started using PV systems to generate electricity in space from The Sun as an alternative energy generation method standalone or together with Radioisotope Thermoelectric Generators (RTGs) which was used in Voyager 1 satellite that was passed the limit of Solar System in 2012. Since, an aircraft can be moved by some forces that can be produced by electrically powered propulsion method, PV panels have become more important. In this method the electricity used to create a force with supplement fuels. Moreover, PV panels also supply electricity for heating-cooling of satellites, their sensors and measurement tools. Thus, it became crucial for spacecrafts and it has been suggested that more than half of the satellites of Russian space industry will carry PV panels after 2020.

PVT system, which is a combination of simple heat exchanger and PV panel, has been used to transform solar energy to both heat and electricity. Because PV panels do not generate electricity with constant efficiency. Their efficiency changes according to panel temperature. For this reason, pipes carrying a heat transfer fluid such as water attached to the back of PV panel. These lead to the enhancement of

efficiency of PV panel because water absorbs the excessive heat of PV panel from its back and keeps it at an optimum level of temperature for electricity production.

1.3. Solar Thermal Systems

Water heating systems is crucial for both industry and daily living to enhance the temperature of the water to a specific degree to make it ready to use. Many ways of accomplishing this purpose are available. One cost effective and renewable way is to use solar energy. Solar Domestic Hot Water (SDHW) systems referred to as solar water heating systems and have been used for a long time. In the past, in order to heat water, fossil fuels were used commonly like coal and so the places which have not fuels were not capable of using hot water. Using solar energy as a location independent resource is a means of heating water. Another advantage of this method is that it is easy to use. Although it is available almost any location on the surface of Earth, it is not ready to use resource all the time of the day due to the rotation of the Earth.

In a small surface area, most water heating systems cannot heat water to a required level in a short time such that it takes for hours until afternoon. These drawbacks led to the improvements of solar water heating systems by attaching an energy storage system like a water tank to preserve heated water from the time in which the collector is operating till the time when water temperature level reaches a unwanted degree. Thus, the main goal of the solar collector is to feed the tank as much as possible. This also decrease the maximum temperature point of water but increase the time of available hot water. Because if tank is not attached, the solar radiation receiver which is also known as collector can heat less water inside to a higher temperature degree but cannot provide necessary amount of water.

Although, the tanks that were used first for this purpose increased the amount of water in the system together with collector, it was not good enough to keep the hot water for longer periods since it was not insulated well. After the first demonstration of the basic solar collector as a water heating system in 1891 by Clarence Kemp, it had not been changed until 20th century. What's more, it was neither a split nor an insulated system therefore it was highly vulnerable to the weather conditions.

The first solar collectors that was ready to use for both day and night was invented by William Bailey in 1909. This design was allowing the water staying hot whole day because the tank was insulated to keep water hot inside tank. However, heat losses were occurring even the insulation was used. The water was being circulated inside the system from the collector to the tank in a natural way consecutively. In conclusion, an actuator was not required in this system.

As it was well known that the glass is a good transparent solar radiation transmitter and a poor absorber, it was used to cover the solar collector to not resist sun rays over the absorber plate.

In 1950s, some countries such as Japan and Australia were installed hundreds of solar water heating systems having basins. Until 1980s, more than half of the population of Israel were using solar energy to heat their water and recently this amount was exceeded 90%. The government motivated the inhabitants to use solar energy for water heating after the increase in oil prices.

Greek started using solar water collectors by ordering the first products from Israel in 70's and the Greek Solar Association was established in 1978 afterwards.

In Australia, the increasing period of using solar water heating systems were disrupted by the usage of natural energy at locations where fuel is inadequate.

1.3.1. Flat-Plate Solar Collector

Solar water heating is an integral part of life. There are many systems to heat water. One common type of solar water heating systems is flat-plate solar collectors which is utilizing solar energy. They have been designed by changing materials, manufacturing ways, dimensions and designs of connecting apparatus, pipes, insulation, absorber plate, glasses.

Flat plate solar collectors contain an absorber plate which has the ability to minimize emittance (ϵ) and maximize the absorptance (α) and transmittance (τ) as much as possible in order that the absorber plate can absorb the incident radiation and transfer it as heat to the pipes in which a working fluid flowing.

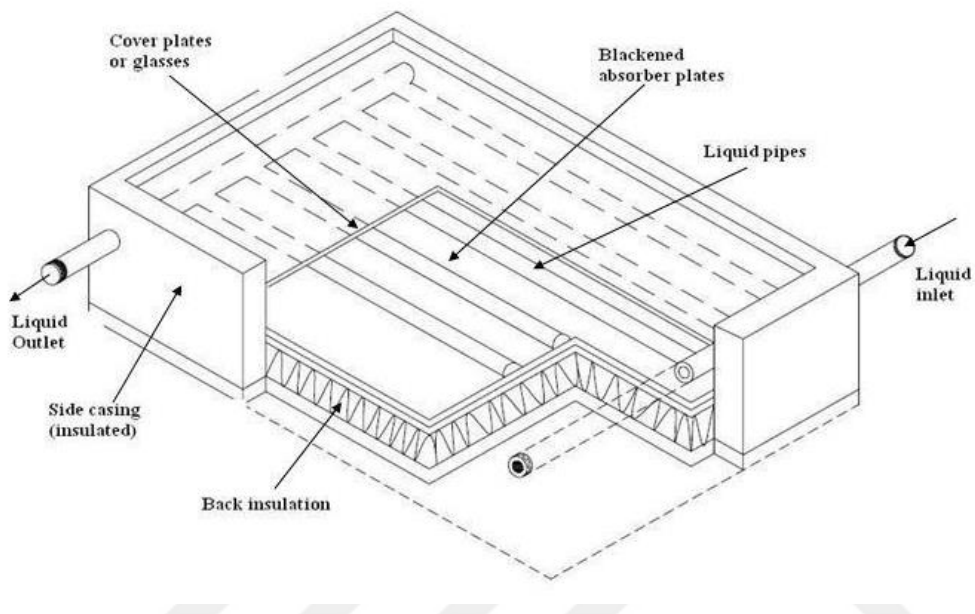


Figure 1.5 Cross sectional view of the common flat-plate solar collector(Singh, 2014)

A cross sectional view of the most used flat-plate solar collector can be seen in Figure 1.5 . A common type of flat-plate solar collector basically includes one or more glass cover. These covers must have the ability to transmit the sun's rays to the absorber plate. Thus, it must have the capability to low absorptance and emittance but high transmissivity. Therefore, the glasses used as a cover of FPSCs transmits more than 90% of the sunlight to the absorber plate. However, if more transparent glasses are used, the radiant heat that is reaching the place is reduced. But the heat transfer by convection from the plate to the ambient through the air in the apertures between plate and glasses is also reduced thus decreasing the convective heat losses.

The absorber plate emits the heat by radiation to the environment through glass since the absorber plate temperature is higher than that of ambient. Glass covers, however, accepted as transparent and they reradiate to the environment due to the same heat transfer rule.

Flat-plate solar collectors can also be produced without glazing. Here, the main aim is to prevent radiative and conductive losses by means of glass cover , whilst, this method allow excessive convective losses from absorber plate to the cooler air

outside and it also vulnerable to the environment conditions such as rain, dust, insects and animals, etc.

In order to reach better efficiency values, absorber plates with selective surfaces have been used. Nowadays, selective surfaces are of good transmissivities ranging between 90 to 98% and good emissivity ranging between 3 to 10% are in use.

The wavelengths of the sunlight inside the atmosphere and outside the atmosphere are vary. Approximately half of the extra-terrestrial sunlight absorbs and emits to the space by atmosphere. Thus, the remaining sunlight then reaches the surface having both short and long wavelengths. Short wavelengths with higher frequencies have higher energy levels compared with long wavelengths which have lower frequencies to move the electrons in semiconductor junctions. In other words, the visible light in nanometer size ranging from Ultraviolet to Infrared (380 nm – 750 nm) is enough for PV cells. Additionally, the recent studies show that the wavelength range which is necessary to generate electricity in PV cells can be increased by the state of art techniques. To absorb short wavelength, which has higher energy and frequency, the surface of absorber and even the side and bottom areas of the whole FPSC painted black or selected as black material. This provide higher efficiency because the radiative losses are lowered. In short, the absorber plate can absorb 95% of solar radiation coming from the atmosphere.

Another design parameter for flat-plate solar collector is to choose materials that can endure the high temperature up to 200 °C aside from the properties mentioned above. This is an important parameter that must be considered when selecting all parts of the FPSC.

Collector pipes are also important as a bridge for transferring heat between FPSC and liquid. This is crucial because the goal of using FPSC is to heat water. Therefore, pipes carrying the fluid spaced not more than 10 cm apart in many systems as the heat could be already lost before even reaching the pipes on the absorber plate attached.

The heat losses from FPSCs are also caused by the tilted surface from the horizon thus the beam radiation cannot be taken perpendicularly all day and some radiation reflects to the ground and ambient. However, beam radiation is not the only solar radiation type that FPSCs can collect. They can also collect diffuse solar radiation.

Owing to their low costs and simple design, FPSCs have been used more than other solar water heaters until recently. They also used as preheaters for the systems that needs liquids with higher temperatures to work in industry.

1.3.2. Evacuated Tube Solar Collectors

1.3.2.1. Heat Pipe Evacuated Tube Solar Collector

Evacuated tube solar collector with heat pipe as shown in Figure 1.6, has two parallel cylindrical glasses has a gap between them and the gap then evacuated and the air inside causing the convective and conductive heat losses are removed.

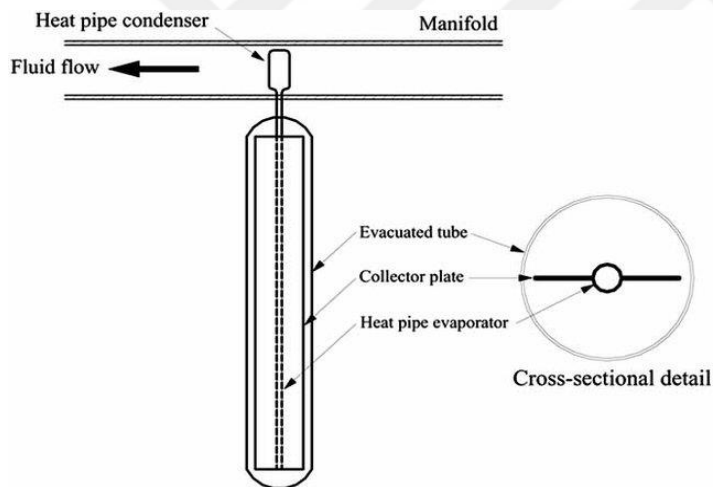


Figure 1.6 Heat Pipe ETC (Kalogirou 2007)

The heat pipe contains mostly water and water molecules adjacent to the inner glass start to evaporate and with natural convection they move up and reach the manifold which is attached to the tank or continuous flow, and realise its heat and condense and become havier again and drops to deeper. Therefore, these movements create a evaporative-condensed cycle naturally and more efficient than FPSCs, because when the water evaporates (phase change), it absorbs latent heat which is higher than the heat absorbed only with temperature change but no phase change. The vapour phase water molecules are also of higher velocities when they stacked inside the water and travel to upward faster. This also increase the natural convection cycle speed thus thermal efficiency. Moreover, the water can start boil at very low

temperature due to low pressure at 30 °C. This is quickly achievable temperature level considering the solar collector types.

1.3.2.2. Direct Flow ETC

Evacuated tube solar collector can be designed to allow working fluid directly flowing inside the circular or plate shaped copper or aluminium. Between the absorber and the glass cover is evacuated. This type of collector is called as direct flow ETC. The efficiency is lesser than Heat pipe ETC because the working fluid may not be boiled quickly. However, if the length of the absorber tube is long enough to heat liquid to a level which is allowing fluid to boil at low pressure. A schematic drawing of Direct Flow ETC can be seen in Figure 1.7.

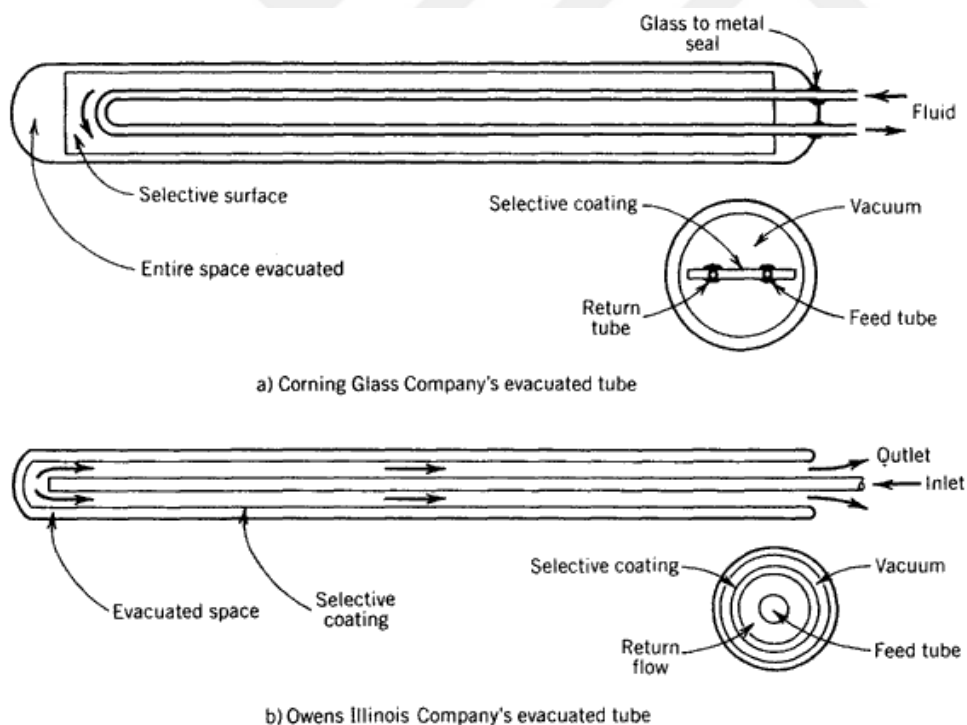


Figure 1.7 Direct Flow ETC(Stine & Geyer, 2001)

1.3.2.3. Thermal Tube Collector (TTC)

Thermal tube collectors have similar working principles like other evacuated tube solar collectors; however, there exist a heat exchanger in the header tank and heat

transfer fluid in absorber tubes which is evacuated. A typical Thermal tube collector can be seen in the Figure 1.8.

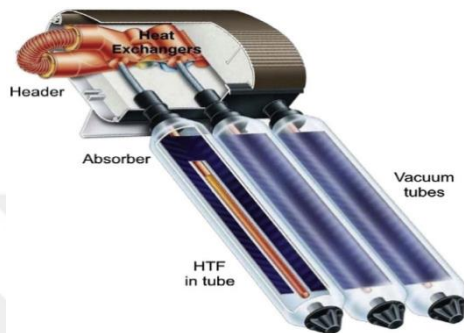


Figure 1.8 Illustration of thermal tube solar collector (Sarbu & Sebarchievici, 2017)

1.3.3. Solar Air Collectors

Solar air collectors are similar to flat-plate collectors but the working fluid is air. As it can be seen in Figure 1.9 that the collector contains an absorber plate and has a glass or selective transparent cover. The air between plate and glass is isolated from the ambient air and can be used for air conditioning such as space heating. Air has lower thermal conductivity than that of water and thus requires fans with higher power. This decreases the efficiency of solar air collectors. If the solar air heaters wanted to be used without actuator to create flow, they should be tilted to a certain degree so that air heated can rise up and create a circulation by natural convection.

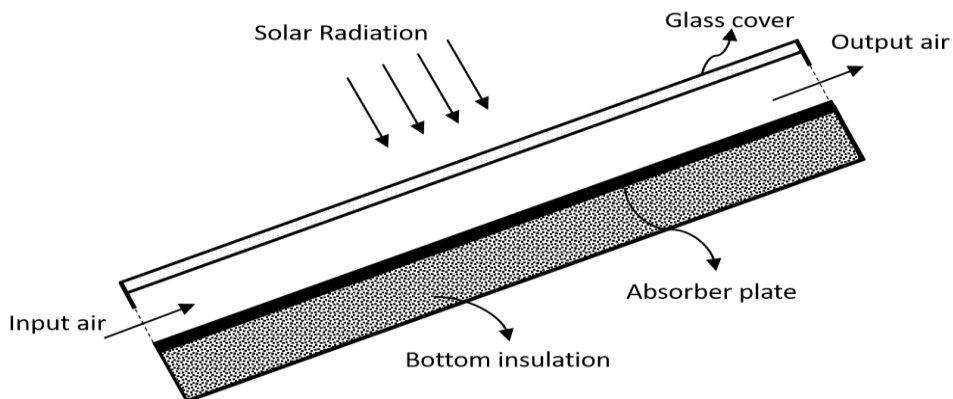


Figure 1.9 Solar air collector

Solar air heater collectors are of similar design to that of liquid heater collectors. Absorber plate of the air heaters comprised of screen layers, metallic or non-metallic materials. In Air collectors, forced or natural convection of air circulation ways can be used. Forced convection can be preferred when the natural air circulation inside is lower than the desired level. Moreover, if the air flow is to be turbulent and faster, the heat flux increases from the collector to the air while it is passing through the air collector. However, if the objective of using this design is not for place heating, it should not be selected, because the air absorbs and transfer heat takes place with lower efficiency compared with liquid. Plus, for forced convection a fan has to be attached or used together with the system.

1.3.4. Concentration Solar Collectors

Concentrating solar collectors have better thermal efficiencies than non-concentrated solar collectors thanks to their higher concentration ratios. They have different types of concentrators which are produced to increase the concentration ratio by means of refraction or reflection. They can be classified as imaging or non-imaging according to position.

1.3.4.1. Parabolic Trough CSC

A schematic drawing of stationary parabolic trough concentrating solar collector is demonstrated in the Figure 1.10. The system contains parabolic reflectors that

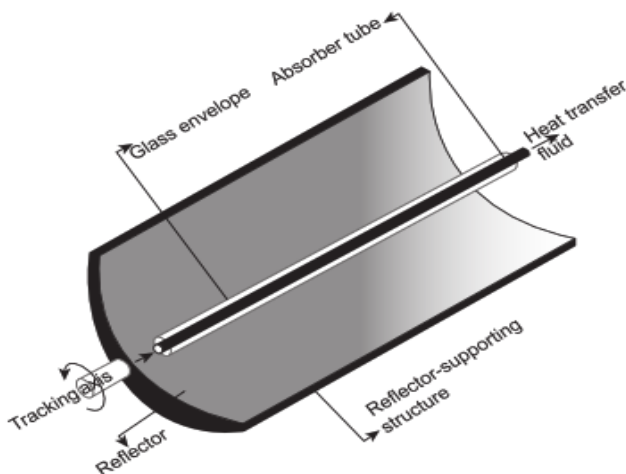


Figure 1.10 Schematic of Parabolic Trough Concentrated Solar Collector

reflects the sun rays onto the absorber tube. The reflector can also be comprised of flat reflector surfaces when the absorber plate diameter is bigger or the flat reflectors are of small widths and projected to the absorber tube. The acceptance angle is expressed as the ability to obtain light while attached to the system. Thus, having a broad range of light welcoming area increases the acceptance angle of the collector and allows the system to be more efficient than other stationary solar collector types since it has no need to be attached a sun tracker mechanism, and yet can be stationary. Three types of common stationary solar collectors are demonstrated below. Today, larger scales of stationary parabolic through solar collectors are in use. A novel design has reached the 7.6 meters high and 150-meter width sizes. By this design the cost decreases by 20 percent and working fluid temperature reaches up to 550 °C.

1.4. Solar Energy

1.4.1. Solar Radiation

Renewable energy resources directly or indirectly originated from the Sun which is accepted as constant infinite resource. This chapter, the intensity and spectral distribution of the incident radiation will be considered. The solar energy with wavelength between 0.25 and 3.0 micrometer which is most of the solar radiation reaching the imaginary surface just before entering the atmosphere. Since the radiation coming to the earth surface changes depends on Earth position and orientation around the world and the environment surrounded, the location of the Sun in the sky, the direction of incident beam radiation and shading are to be examined. These subjects together with extra-terrestrial radiation which is the theoretically the upmost solar radiation limit that a surface can receive will be revealed in second section of this chapter.

Knowing the extra-terrestrial radiation, surface location and orientation and available radiation on outside of the surface of earth is crucial for understanding the concept of solar radiation and obtained data.

1.4.2. The Source of Solar Energy

The Sun with a diameter of 1.5×10^{11} times than that of the size of Earth present at the centre of the Milky Way Galaxy. The Sun complete its revolving in 4 weeks. But, Earth completes the rotation in different time periods. The Polar Regions of

Sun complete the revolution in approximately 30 days and the rotation of equator takes roughly 27 days. The Sun's temperature vary at different locations over various diameter. Besides, the temperature of the sun is accepted as effective blackbody temperature of 5777 K. However, the information that we have regarding internal regions of the Sun is uncertain and we have only estimated value ranging between 8×10^6 and 4×10^7 K. As a fusion reactor, The Sun, supplies a radiative energy. While this fusion reaction takes place, four protons assemble and compose helium nucleus. However, the mass of helium nucleus become lesser. The reason because of the mass decrement is explained with the energy output during the fusion reaction in the Sun.

An intensive energy produced in the central region of The Sun as the temperature of millions of degrees exits out of the Sun changing. The radiative and convective processes take place simultaneously by absorption, emission and reirradiation. The Sun's core radiates X and Gamma rays. Radiation wavelength is higher when the temperature is lower. So, the larger the distance from the centre of The Sun, the higher the wavelength of the radiation. Two fifths of the mass of the Sun situated the radius from 0 to $11.5D$ (D is the diameter of the sun) and nine tenths of the energy created in this region. 130000 K is estimated at the distance of $35D$ and the density has decreased to 70 kg/m^3 . From this point to larger diameters, the convective process becomes crucial, thus the layer from $30D$ to $50D$ called as convective zone. In this zone the temperature decreases to approximately 5000K and the density drops to 10^{-5} kg/m^3 . Irregular convection cells ranging between 1000 to 3000 km size and their lives last only a couple minutes known as granule composition at the Sun's surface. In solar surface some small dark areas known as pores and their size similar to convection cells. On the other hand, bigger and various size of dark regions named as sunspots. Outer convection layer region known as photosphere. Going further along the stretch of the same line, another layer appears and is called as photosphere having a sharp edge. But, its density is low compared to that of air at sea level (roughly one ten thousandth of air). This layer is not transparent and with ionized gases. This feature allows radiation to be absorbed and emitted in continuous spectrum. During the solar eclipse, outside the photosphere can be seen since it is semi-transparent solar atmosphere. After the photosphere, the layer of hundred kilometres deep with gases cooler than previous layer referred to as reversing layer. The outer layer of reversing layer is called chromosphere which is thousands kilometres deep (roughly 10.000 km).

Chromosphere filled with gases having lower density and higher temperatures than photosphere. The corona appear in outside of the Chromosphere with the lowest density among all layers of the sun, but having a very high temperature of 10 million Kelvin.

Now that the simple physical structure, temperature, density radiant of the sun explained above, it can be concluded that the sun cannot be seen as a blackbody at a constant temperature. Instead, the emission and absorption of the radiation with different wavelengths of layers of the sun forms the total emitted radiation as a whole. The total extra-terrestrial solar radiation and spectral distribution of it can be measured by several methods in various experiments. The results will be interpreted in following sections.

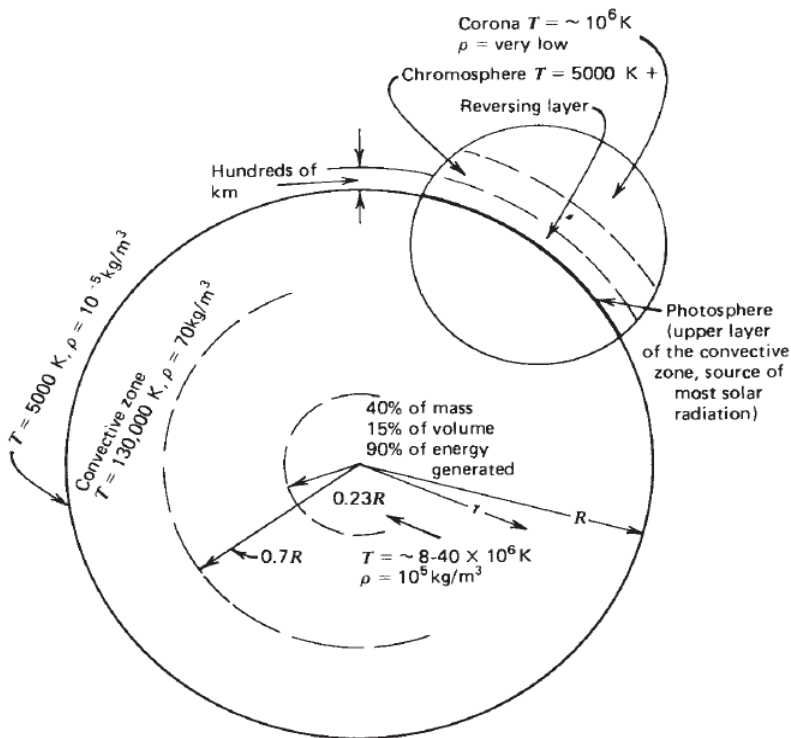


Figure 1.11 The structure of the Sun (Duffie et al., 2013)

1.4.2.1. The Solar Constant

The astronomical unit (AU) is referred to the distance from the center of the sun to the center of the earth. Although this distance varies by 1%. International Astronomy Union (IAU) fixed this number as 149,597,870,700 meters and this unit used to express huge distances between space objects. It can be rounded to roughly 1.49×10^{11} meters. The total radiation reaches on per unit of area on the surface of outside of the earth atmosphere at the mean distance between the sun and the earth perpendicular to the sun rays per unit time is referred to as the solar constant (G_{sc}). The illustration below shows the eccentric sizes of the earth and the sun and the way on which the radiation reaches the earth.

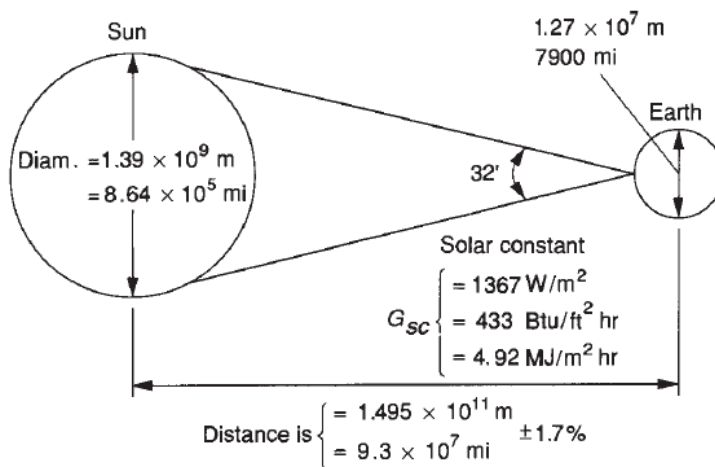


Figure 1.12 Geometry of the solar constant (Duffie et al., 2013)

The solar constant measurements or estimations were done until the time in which the spacecrafts are available on the space. The estimations were done on the surface of the earth, mostly on top of the mountains at which the solar radiation is less transmitted through the atmosphere and partially emitted and absorbed by the materials in the sky. On the grounds that the estimations only based on the terrestrial measurements and its extrapolations, this led to the wrong calculations of the solar

constant. The solar constant was measured by C.G. Abbot et.al. (1954) as 1322 W/m^2 then defined by Johnson as 1395 W/m^2 .

The further studies made with the help of balloons and aircrafts at high altitudes and thus the results obtained from direct measurements on the whole the World surface. The solar constant was changed to 1353 W/m^2 and NASA accepted the value in 1971. The American Society of Testing the Materials also admitted the value in 2006.

The solar constant values of 1373 W/m^2 (Fröhlich, 1977; Hickey et al., 1982), 1368 W/m^2 (Wilson, 1962) $1367, 1372, 1374 \text{ W/m}^2$ (Duncan et al., 1982) as cited in (Duffie et al., 2013) were measured by different methods. The solar constant was accepted by the World Radiation Centre with a correction of 1% as of 1367 W/m^2 . This constant used in many studies and books. Based on one of the latest study done by Gueymard (2018) the solar constant can be accepted as 1361.1 W/m^2 according to the data which can be seen from Figure 1.13 received during the last 42 years from 1976 to 2017.

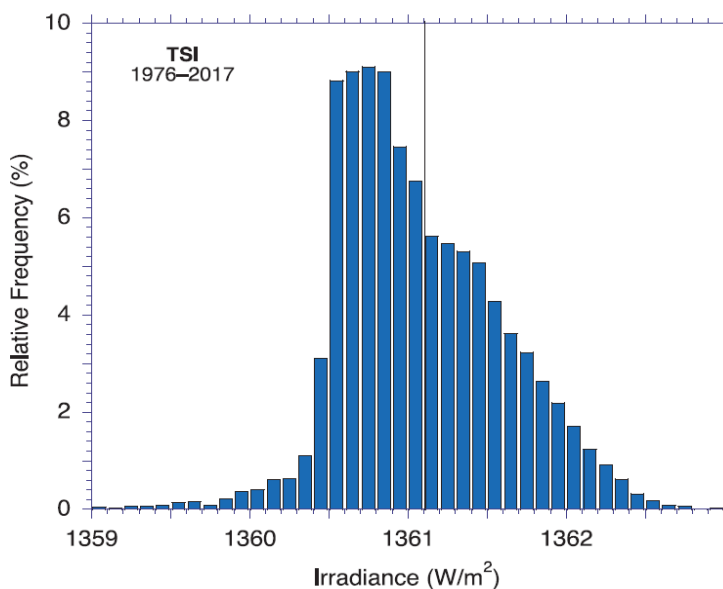


Figure 1.13 The total solar irradiance in the years between 1976 to 2017. The black vertical line shows the solar constant (Gueymard,2018)

1.4.2.2. Fluctuation of Extra-Terrestrial Radiation

The solar radiation available out of the atmosphere of the earth varies due to two reasons. First, according to the data obtained from different studies, the results are not fit to each other. However, the differences between the results are not more than 1.5%. Moreover, the data collected by Hickey et al. (1982) during two and half year starting in 1982 demonstrate the decline in solar energy by 0.02%. But, the solar energy changes owing to the sunspots and conflicting reports should be ignored and fixed a mean value so as to substituting into formulations in engineering. The second but the one should be taken into account as a fluctuation is due to the distance between the earth and the sun. Such that, the data of the solar radiation fluctuate at best 3.3% over the year.

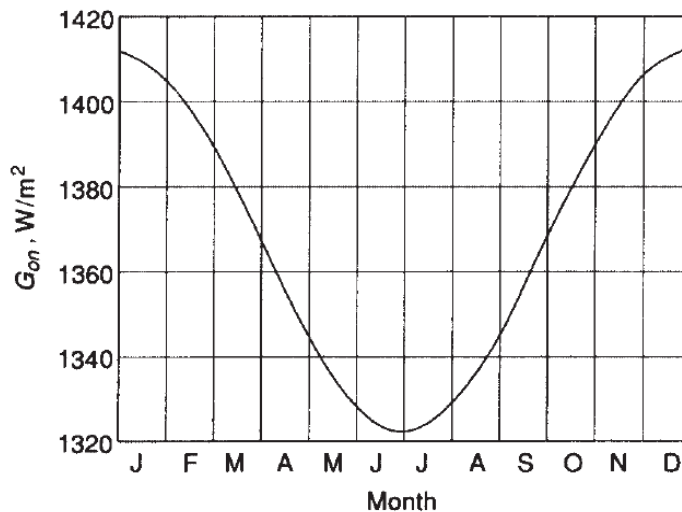


Figure 1.14 Monthly Solar radiation over the year

Spencer (1971) derived an equation to simply calculate the solar radiation depending on a year.

$$G_{on} = G_{sc} \left[1 + 0.033 * \cos\left(\frac{360n}{365}\right) \right] \quad (1.1)$$

Where G_{on} is referred to as incident extraterrestrial radiation on a place which is normal to radiation on the n^{th} day of the year. This equation has been used in many

engineering applications and fairly accurate. Second version of calculation of solar energy was given as

$$G_{on} = G_{sc} [1.000110 + 0.034221 \cos(B) + 0.001280 \sin(B) + 0.000719 \cos(2B) + 0.000077 \sin(2B)] \quad (1.2)$$

Where B is expressed as

$$B = (n - 1) * \left(\frac{360}{365}\right) \quad (1.3)$$

1.4.2.3. Types of Solar radiation

Air Mass (m) depends on zenith angle and at sea level it is 1 and at 60° of zenith angle it is 2. For the zenith angle in the 0°-70° angle range

$$m = (\cos\theta)^{-1} \quad (1.4)$$

Another equation based on empirical studies applicable while zenith angle is close to 90°

$$m = \frac{\exp(-0.0001184h)}{\cos(\theta_z) + 0.5057(96.080 - \theta_z)^{-1.634}} \quad (1.5)$$

Where h is defined as site altitude as metre

Beam Radiation is the pure radiation coming from the sun just before entering the atmosphere. This is also called as direct radiation. Diffuse Radiation, on the other hand, is the sky radiation which diverted from the beam radiation after scattered by clouds in other words mainly by the water molecules in air. Total solar radiation is the sum of diffuse and beam radiations. As shown in the figure below, overall solar radiation consists of three types of solar radiation on a horizontal surface.

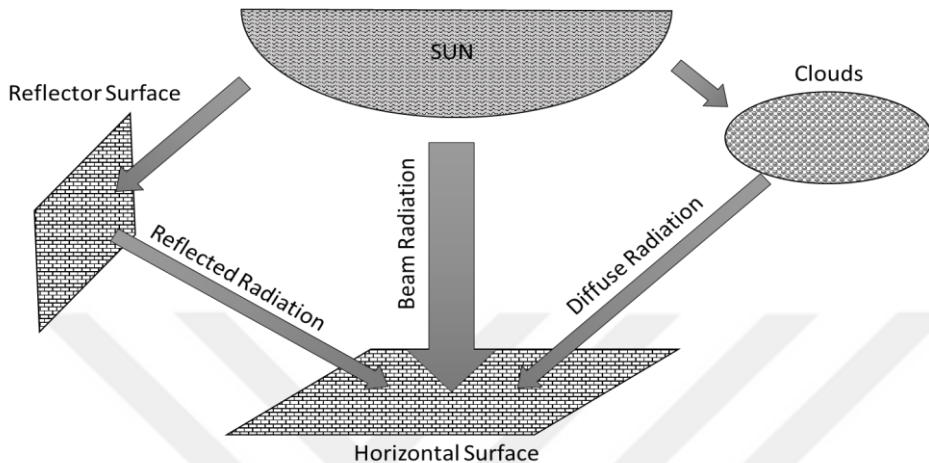


Figure 1.15 Total Solar Radiation as the sum of beam, diffuse and reflected radiation.

1.4.2.4. Angles and Directions of Solar Radiation

As with all distant objects, location and relative location determination terms are to be explained here. In this case the Sun's rays after touching the atmosphere will be identified by related terms. The direction of beam radiation will be determined, while diffuse radiation direction will not, due to its instant change depending on surface location, clouds, altitude, weather conditions etc. But diffuse radiation intensity can be calculated by various ways.

In solar energy, the angle, intensity, direction of the incident radiation are crucial for determining absorbed solar energy. Because, all locations in the world acquiring the solar radiation with different angle, time, duration, intensity etc. Therefore, some common angles and terms are defined to calculate incident solar radiation.

Latitude (ϕ) is the location with an angle from equator in both north and south direction to be at most 90° and -90° , respectively.

Declination (δ) angle represents the position of the sun while it is on the local meridian with respect to the surface on the equator. It stays in the range of -23.45° and 23.45° .

Slope (β) is the deviation of the surface from the horizontal surface on the same location. The slope range is from 0° to 180° and so 90° means the plane is vertical.

Solar azimuth angle (γ) is expressed as the angle between the imaginary line from the center of the sun hitting to the normal plane on surface which is due South and it changes in a range $180 < \gamma < 180$.

Hour Angle (ω) is the angle which represent how far the obserber's meridian to the pole of the earth and expressed by hours and minutes, which 15° is one accepted as one-hour negative until 12:00 am after this time it is positive.

Incident angle (θ) is the angular displacement between the beam radiation coming onto a surface and its normal. Incident angle modifier is a correction factor for tilted planes.

Zenith angle (θ_z) is formed between the beam radiation on a surface and normal of the the surface.

Solar azimuth angle (γ_s) is the angle between projection of the sun due south on a plane horizontal on earth surface.

Solar altitude angle (α_s) is the angular displacement from horizon to the line coming from Sun and completes the zenith angle

1.4.2.5. Solar Time

The sum of these two solar radiation types (the radiation reflected from other surfaces on earth mostly ignored) reaching on a surface defined as total solar radiation. The total solar radiation is also called as global radiation. Incident radiant energy on a surface area referred to as irradiance (W/m^2) depicted with "G" and subscriptions such as b(beam), d(diffuse), s(spectral) on it demonstrates its radiation type. Similarly, irradiation which is also known as Radiant Exposure (J/m^2) is found by integrating irradiance over time. In the literature of solar energy, time is expressed as hour or day rather than defined as default unit second (s).

The solar energy can be expressed by the letters I an H, for hour and for day, respectively. They can also show beam, diffuse and spectral radiation on any surface if they used with subscripts mentioned before. Insolation which is mostly used in

solar energy used with these two letters. Radiant Existence or Radiosity (W/m^2) is the name of the energy transfer rate in terms of radiation heat transfer types such as emission, reflection or transmission of an area of surface in meter square. If the energy is only transferred by emission on a surface, it is called emissive power.

Rather than insolation terms (I and H), the all radiation terms mentioned above can be used for any wavelength range or monochromatic radiation. But, I an H terms only used for solar energy spectrum. Solar time and local time are differ from each other and some corrections needed. These differences can be found by applying following equation

$$\text{Solar Time} - \text{Standard Local Time} = E + 4(L_{sm} - L_{lol}) \quad (1.6)$$

Where L_{sm} is the standard meridian at the local time zone and L_{lol} indicate the longitude of locaiton. The longitudes are expressed in degrees in the range between 0° and 360° (West direction). And E which is the equation of the time formulated as

$$E = 229.2(0.000075 + 0.001868 \cos(B) - 0.032077 \sin(B) - 0.014615 \cos(2B) - 0.04089 \sin(2B)) \quad (1.7)$$

E can be determined from Figure 1.16.

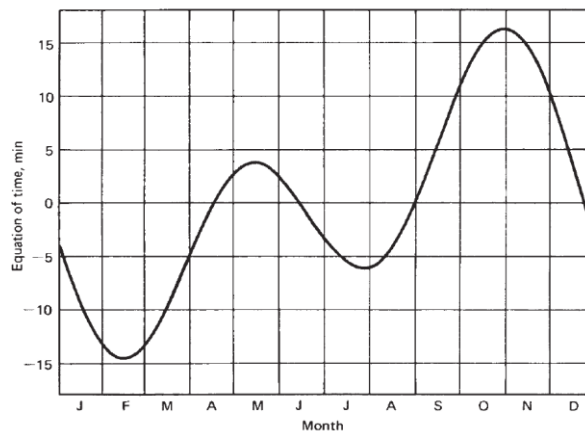


Figure 1.16 E values in minutes during the year

2. LITERATURE REVIEW

2.1. Review of Nanofluid

Contemporary life in which being faster, smaller and compact has become compulsory. Therefore, thermal systems are needed to fit any systems where they are in use in terms of their size and usability. Thermally enhanced fluids are in need of processes mainly for heating and cooling of from large areas to tiny electronic parts because of insufficient efficiency of conventional working fluids. It is well known that metallic particles are of great thermal conductivity. Knowing that their superior thermal properties, they have been considered to use in a fluid which is acting as a carrier. Micro scale metallic particles have used to increase efficiency of the thermal systems. However, the require for enhancing thermal efficiency has conveyed researchers to seek smaller size of particles since mili or micro scale particles cause considerable amount of pressure drop and viscosity increments. This led to power increment of needed for the system. If the system is working with forced convection this issue becomes a problem is to be taken care of. Another parameter is to be considered is the life of the system in which heat transfer fluid is used is also important. Heat transfer fluids (HTF) are used for the fluids commonly mixture of two or more fluids prepared by various methods so as to increase heat transfer properties of the working fluid thus increasing the performance of the system. However, heat transfer fluids are not only have better thermal properties, they also increase the life of system by preventing pump stockings thanks to their unique material properties in the closed systems.

Nano particles dispersed in a base fluids and formed as a solution is named as Nanofluids first by Stephan Choi. Nanofluids which includes nano scale particles in the range of 1-100 nm have better thermal properties than those of conventional fluids (Choi & Eastman, 1995) . Nanofluids are used in earlier times for cooling as a working fluid in heat exchangers (Kumar et al., 2015). Heat exchanger is a material by which heat can be transferred from one point to another. In a heat exchanger one or more different types of fluids can be used according to the heat exchanger design. Heat exchangers are used for adjusting the temperature of the system as a form of a device or a material (Kumar et al., 2015).

Considerable amounts of attempts have been made to enhance thermal properties of fluid and mainly metallic nanoparticles used due to their high thermal conductivity.

Nanofluids are chosen due to their effects on thermal properties by altering relative surface area and quantum effects that change their physical, chemical, electrical, optical and magnetic features (Das, 2017). Moreover, nanofluids containing nanoparticles are of great attention when choosing as a working fluid owing to tiny particles size and large surface area. Because, it is well known that higher amount of heat flux takes place on a surface which is greater than other when the all conditions are assumed as the same.

Hybrid Nanofluid is a fluid which consists more than one nanoparticle (Dhinesh Kumar and Valan Arasu 2018) .Nanoparticles have suspended to form a homogenous mixture to comprise of their both physical and chemical properties. So, a synthetic hybrid nanofluid has better psychochemical features than that of nanofluids which include only one type of nanoparticle(Suresh et al., 2012). Studies have done for evaluation nanofluid, which contains one type of nanoparticle, by experimental, numerical and theoretical ways demonstrate that they have great potential usage in cooling cameras, electronics, micro devices, heat exchangers, spacecrafts and fuel cells etc. (Li et al., 2009) .

2.1.1. Synthesis of Nanofluids

The methods of preparing nanofluids can be classified under the categories: one step and two-steps method. The differences between these two methods are transportation, cost and flexibility in terms of forming various nanofluids. Although nanofluids synthesized by using one step method is more stable, not all the sizes or types of nanoparticles can be tried in the base fluid. Therefore, more economic and transportation friendly way was found. Two step method allows many nanoparticles with different sizes dispersed in various base fluids with different sizes and shapes. Thus, it is mostly used in preparation of nanofluids.

2.1.1.1. Two Steps Method

The most common method for preparing nanofluids is two steps method. As with every method it has advantages and disadvantages. Depending on the aim of the study, nanofluids can be customized. In this method dispersion and preparation of nanoparticles are separated. Procedure for preparing the nanofluid starts with preparing nanoparticles as powder form. Then, this nanopowder mixed homogenously in a base fluid using various methods. A disadvantage of this method

which is an undeniable problem for nanofluid prepared by two step method without a dispersant is agglomeration in a very short time. Thus it becomes a fluid which shows better thermal properties for a limited time that is not useful for any system. Researchers mostly use dispersants, which is an additive and alters the physical and chemical properties of nanofluid and unpredicted effects take place, and they keep the dispersing duration longer while preparing nanofluids. So, nanofluids stay stable for longer periods and can be used in a system. However, nanofluid sedimentation and agglomeration are the problems that have not been overcome yet. A typical two steps method in preparing nanofluid can be seen from the figure below. Ultrasonication is a common method used together with dispersant addition in order to reduce agglomeration. Dispersant is a product that changes the mid-layer structure between base fluid molecules and nanoparticle surface. This also changes the zeta potential which is a proved parameter affecting the agglomeration of the particles in the base fluid.

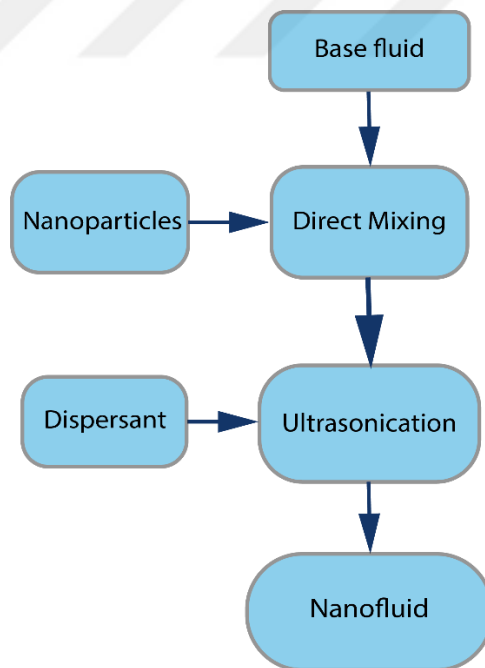


Figure 2.1 Preparation of nanofluid by two steps method

2.1.1.2. One Step Method

Another well-known method for preparing nanofluid is synthesizing at once is called as single step method. Results obtained from various studies applied one step method for synthesizing nanofluids are not in good agreement. This is because single step method requires low vapour pressure and a process in which nanoparticle preparation and dispersion occur simultaneously.

With one step method agglomeration duration is prolonged by eliminating the transportation, drying and dispersion of nanoparticles. Physical vapour condensation method has been used to prepare nanofluids such as Cu/EG by many researchers.

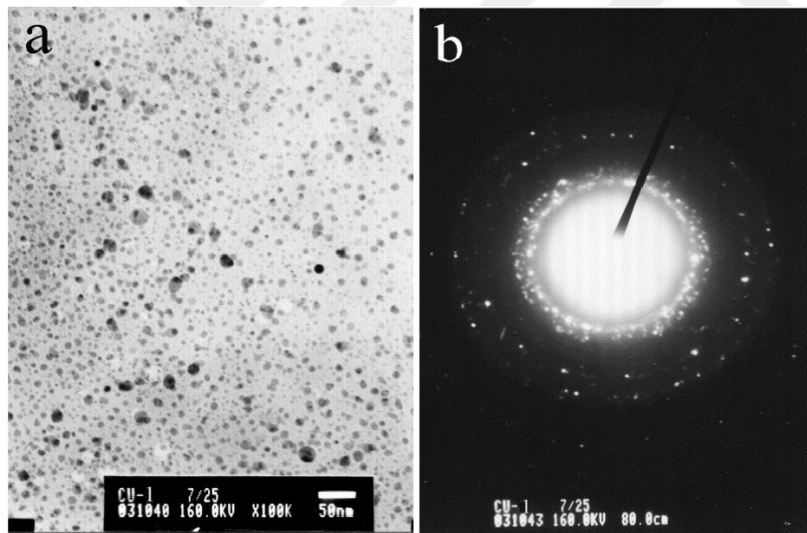


Figure 2.2 TEM image of Cu nanofluid prepared using one step method (Zhu et al., 2004)

A typical Cu nanofluid prepared by a novel chemical one step method which includes magnetic stirring can be seen in Figure 2.2.

2.1.2. Types of Nanofluids

There are many types of nanofluids used various preparation methods, base fluids and nanoparticles. These nanofluids can be listed as

- Ceramic nanofluids: copper oxide, aluminium oxide, titanium oxide, zinc oxide nanofluids
- Magnetic nanofluids
- Metallic nanofluids: copper, gold, silver, nanodiamond, carbon nanotubes, hybrid nanofluids

2.1.3. Thermal Conductivity Measurement Methods

To date various methods have been developed and introduced to measure thermal conductivity of the nanofluids but predominantly transient hot wire method and thermal constant analyser have been used. Other methods such as steady state parallel plate and 3ω method are in use.

2.1.3.1. Transient hot wire method

For the most accurate results given methods as suggested by Horrocks and McLaughlin (Horrocks & McLaughlin, 1963). In this method, a thin long metallic wire method has been mostly chosen as platinum electrically powered in order to make a resistance and a temperature sensor attached to it. This double wire, submerged in a fluid which is to be measured with another temperature sensor submerged in the same fluid. By doing this, electrically powered wire release heat at a certain temperature degree to the surrounding liquid whose temperature measured by other temperature sensor by conduction. The advantage of this methods it knowing exact temperature of the two points and thus evaluating the thermal conductivity by using equations revealed in studies done by (Hammerschmidt & Sabuga, 2000) . This method claimed to be accurate up to 95-100 % according to the studies. Transient How Wire (THW) technique can be seen in Figure 2.3.

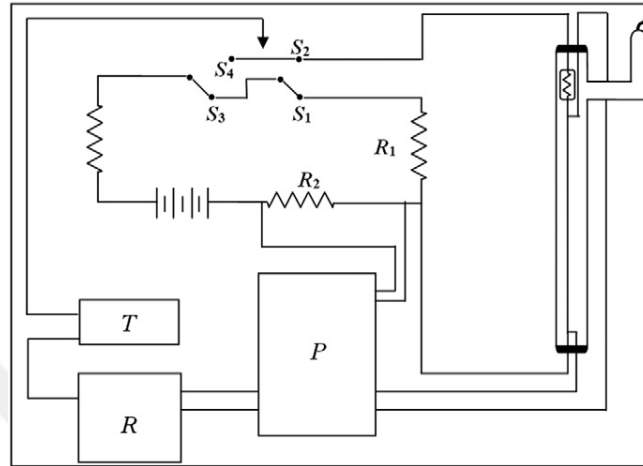


Figure 2.3 Schematic drawing of common hot wire cell and the related electrical circuit(Das, 2017)

2.1.3.2. Thermal constants analyser methods

Thermal constants analyser method uses the transient plane source (TPS) theory in order to determine the thermal conductivity of the nanofluids. This method is easy to implement on the experimental system and responds in very short time with high accuracy. It is also used to determine a broad range of conductivity from 0.02 to 200 W/mK. Moreover there is no need to prepare sample whose sizes can vary. Thermal constant analysers have different types of designs including Hot Disk Method. Mihiriete et al. examined in (Mihiriete et al., 2017) the Hot Disk method by using finite element analysis method and compared with the experimental results. They simulated the Hot Disk method and investigated the density of electric current and the field of the temperature of the metallic strip. They concluded that the temperature transient curve obtained from the simulation is similar to that of obtained from experimental results. One of the basic schematic drawing of thermal constant analyser method which uses TCA and including a thermal constant analyser, thermometer, vessel and a bath kept at the same temperature is shown in Figure 2.4. The probe submerged vertically in a vessel which includes nanofluid and a sensor immersed in it to measure temperature. The nanofluid stayed inside the constant temperature bath so that there will be no heat transfer differences owing to the bath temperature. To determine the thermal conductivity of nanofluid the probe is placed and its resistance is measured.

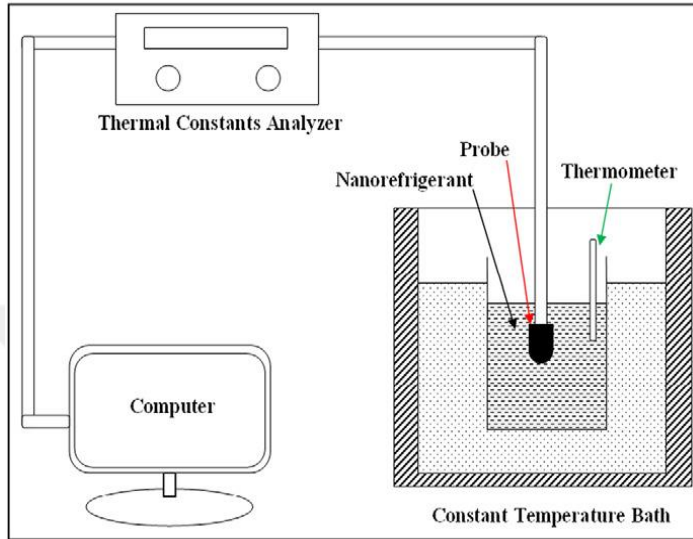


Figure 2.4 Diagram of the thermal constant analyser setup measurement (Das, 2017).

2.1.3.3. Steady-State Parallel Plate Technique

A schematic diagram below demonstrates the steady state parallel plate technique which is developed by (Challoner & Powell, 1956). As can be seen from the experimental setup figure, the test sample is located between the two parallel copper plates rounded and the temperature of the sample determined by each of the thermocouples.

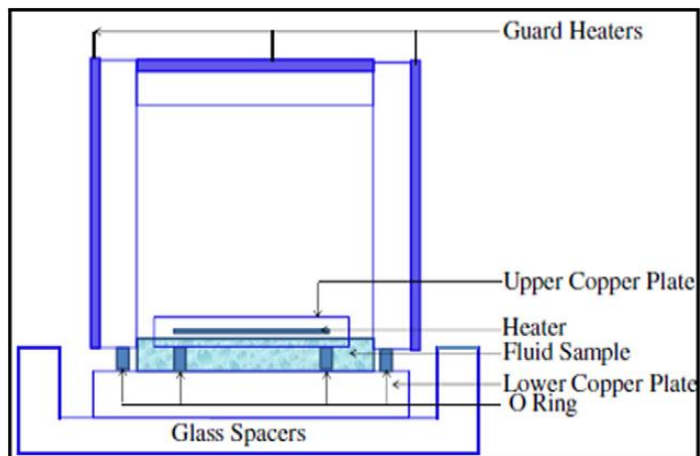


Figure 2.5 A schematic diagram of steady-state parallel plate method

Heater provides heat for the system and then heat transfers through the liquid surrounded and reaches the copper plates placed upper and lower of the heater. The overall thermal conductivity of among the copper plates including glass spacers are calculated by using heat conduction equation then the nanofluid thermal conductivity is found by rearranging the equation according to the unknown thermal conductivity sample which is nanofluid and should to be left or right-hand side of the equation. Heat losses should be avoided in these systems therefore insulations and temperatures controlling techniques are used.

2.1.4. The Effects on the thermal conductivity change of nanofluid

Thermally properties of nanofluids have been investigated by many researchers and parameters and effecting their behaviours in the system by using numerical or experimental methods. They studied on the thermal properties of nanofluids such as thermal conductivity and rheological behaviour that effect their performance. They mainly focused on the parameters such as particle size, particle shape, particle material, volume concentration and temperature. They expressed these parameters are affecting directly the nanofluid thermal properties in the system considerably. Indirectly nanofluid properties during the process has changed depending on other parameters, therefore, in order to determine which parameter is affecting the nanofluid thermal properties considerable amount of studies has to be done. Thus, researchers have studied the parameters below by keeping the all parameters as much as stable but except one or two parameters which is under examination.

2.1.4.1. Particle Size

Considerable amount of studies in literature show that the sizes of nanoparticles are affecting the thermal conductivity of the nanofluid. Such that, when the nanoparticle is of lower size its surface area to volume ratio is greater comparatively, therefore the larger surface area of particle the higher the thermal conductivity. Moreover, the mechanisms such as Brownian motion and particle clustering affect the nanoparticle behaviour more when they are in smaller sizes. Teng et al. (2010) investigated three different nanofluid which includes Al_2O_3 nanoparticles with 20, 50, 100 nm sizes and reported that thermal conductivity of the nanofluid increases with decrease in nanoparticles size. An increment of thermal conductivity of nanofluids with particle size decrement was reported by Mintsa et al. (2009). They found that Al_2O_3 /water nanofluid with 47 nm size has better effective thermal conductivity than that of 37

nm. In another study carried out by Wang, Xu, and S. Choi (1999) shows the comparison for thermal conductivity of Al_2O_3 nanofluid with 28 nm size particles and CuO nanofluid having 23 nm size particles. It is concluded that CuO nanofluid showed higher thermal conductivity because of its smaller size of nanoparticles.

2.1.4.2. Particle Shape

The shapes of nanoparticles can also affect the effective thermal conductivity of nanofluids. Nanoparticles have been used as spherical or cylindrical shapes until recently. Particle shape was investigated using two different SiC/water nanofluid having dispersed nanoparticles with spherical in 26 nm and cylindrical in 600 nm sizes by Xie et al. (2002) and it is found that thermal conductivity enhanced by 22.6% when the volume fractions of the nanoparticles were 4% and increased by 15.8% with a volume fraction of 4.2%. The results showed that thermal conductivity of the nanoparticles changes according to their particle shape. Cylindrical shape nanoparticles show higher thermal conductivity than spherical ones. The figure below illustrates the effect of volume fraction of SiC nanoparticles with different shapes. As can be seen from the Figure 2.6, effective thermal conductivity enhancement higher when cylindrical shape of nanoparticles used rather than using spherical nanoparticles.

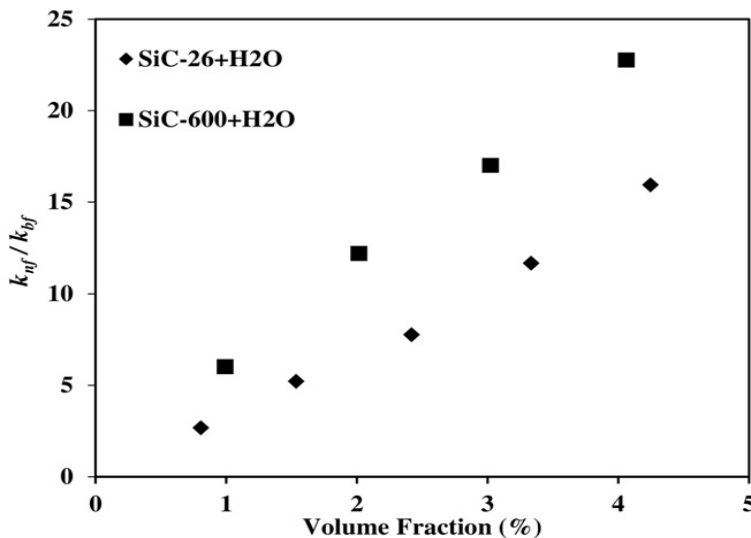


Figure 2.6 Effective thermal conductivity of the two different nanofluids including two different shapes SiC-26 and SiC-600 in DI-H₂O (Xie et al., 2002)

2.1.4.3. Particle Material

Another factor affecting nanofluid thermal conductivity is the material of the nanoparticle. There are many studies focused on the effects of particle materials of nanofluids. It is reported that nanofluid thermal conductivity greatly depends on particle material. As different kinds of nanoparticles dispersed in the same base fluid with the same volumetric ratio shows different thermal conductivities. When nanoparticles with better thermal conductivity is dispersed inside the same base fluid, increases the thermal conductivity of the nanofluid more compared to the nanoparticles with have lower thermal conductivity.

Shima and Philip (2014) found that nanofluid thermal conductivity change can be neglected by nanoparticle material type and it only depends on volume concentration of the nanoparticle. Other researchers, however, who have looked at nanoparticle material effects on the thermal conductivity on nanofluids have found that the kind of nanoparticle affects the thermal conductivity of the nanofluid significantly. Hwang et al. (2006), for instance, investigated three different nanoparticles such as MWCNTs, CuO and SiO₂ dispersed in ethylene glycol and water with the same volume fractions and observed that thermal conductivity of the nanofluid including MWCNTs higher than that of the other nanofluids and they claimed the reason of this effect is because of the fact that MWCNTs thermal conductivity is higher than other two nanoparticles.

2.1.4.4. Volume Concentration

Many studies have been done to investigate whether solid particle concentration in base fluid affects the nanofluid thermal conductivity or not. It can be concluded from studies that nanofluid thermal conductivity is affected by the volume concentration of nanoparticles. Akbari et al. (2017) investigated volume fraction of the nanoparticles effects on heat transfer and found that the heat transfer rate enhanced by increasing volume fraction of the nanoparticles.

Hemmat Esfe (2017) investigated different volume factions of copper oxide-ethylene glycol nanofluid at various temperatures experimentally. The results show that nanofluid viscosity and relative viscosity increased 82.46% with increase in volume fraction 1.5% at 50 °C temperature.

Huminic et al. (2015) made an experimental investigation on nanoparticle volume concentration effect on thermal conductivity of nanofluid and found that increment of volumetric concentration of FeC/water nanofluid results in higher thermal conductivity. Besides, the maximum thermal conductivity enhancement that they reported was at 70 °C temperature with 1.0% volume fraction of nanofluid.

2.1.4.5. Temperature

Temperature affect thermal conductivity of any material more or less. In the case of nanofluid, which is mainly used for enhancing thermal efficiency of the system, it is a significant effect comparatively to conventional fluids. Scientist who have studied temperature effect of nanofluid thermal conductivity have indicated that thermal conductivity of nanofluid depends directly on temperature such that as the temperature increases thermal conductivity of nanofluid increase as well.

+ A study (Mintsa et al., 2009) done to investigate the effective thermal conductivity of Al₂O₃-water and CuO-water nanofluids and reported results show that it enhances with increase in temperature. S. K. Das, Putra, and Roetzel (2003) conducted a study to observe Al₂O₃/water nanofluid with weigh concentration of 1% and reported that its thermal conductivity increases by 8 percent, from %2 to 1%0, with increase in temperature by 29 °C, from 21 to 50. P. K. Das et al. (2017) reported regular increase in thermal conductivity of Al₂O₃/Water nanofluid with increase in temperature.

3. MATERIALS AND METHODS

3.1. Heat Transfer Theory

This chapter covers the theories behind the types of heat transfer. The mathematical background of flat-plate solar collector will be described. The mathematical models then will be used to presume the efficiency of the collector. Relate physical phenomenas, thermodynamic principles, assumptions and ignorances and mathematical models were also demonstrated in this chapter. Fundamentals of heat transfer used to express the theory was explained in (Holman, 2019).

Heat transfer is an energy transfer between two points. Where there is a temperature difference between two or more bodies, heat transfer takes places. Heat t transfer

happens by three main ways in which conduction and radiation are two major definition of heat transfer but convection is a definition derived by conduction equation between a liquid or gas phase material and a solid material. It is a specialized conduction. Thus, it will be mentioned as convection as literature does.

Heat transfer between the bodies always has temperature difference and it is limitless. For example, the solar radiation from Sun to Earth is a never-ending process. Because the temperature of the Sun is always greater than that of Earth. Temperature is a definition of energy locally measured by various temperature measurement tools, or it can be assumed by mathematical approach methods by using a reference point. So, it shows the amount of energy at the measured specific point of body.

While thermodynamics define the heat as an energy transfer way, heat transfer explains both how heat transferred and what the rate of it is. The rate of heat transfer is the main objective of heat transfer topics. Similarly, while heat transfer deals with more complex and detailed and realistic ways of heat transfer rate, thermodynamics only focuses on simplified methods and calculations based on experimental results. What is more, heat transfer takes into account the first and second rules of thermodynamics.

As with kinetics and kinematics in physics the differences between thermodynamics and heat transfer are of similarities. While kinematics only deals with the motion of a body without its creators while kinetics focuses on the forces acting on the body during the motion.

In thermodynamic it can be only described that two different equilibrium of states between two moments of systems. Heat transfer; however, determine at what rate the energy transferred during the process in which the two equilibrium transform from one another.

Proceeding subsections shows the three types of heat transfer types detailed. These fundamental modes will be used to form a total efficiency formula and a general heat equation.

3.1.1. Heat Transfer by Conduction

Conduction heat transfer referred to the situation in which the body that has a temperature gradient due to different temperature nodes. Between these temperature nodes, heat transferred by conduction and the correlation between them expressed as

$$\frac{q_x}{A} \approx \frac{\partial T}{\partial x} \quad (3.1)$$

Heat transfer rate over unit area changes similarly the distance between the temperature nodes and their temperature difference quantity. The temperature gradient is here used as normal temperature gradient.

After inserting the proportionality constant it changes to

$$q_x = -kA \left(\frac{\partial T}{\partial x} \right) \quad (3.2)$$

Where q_x is the heat transfer rate and $\frac{\partial T}{\partial x}$ is the temperature gradient in direction of heat flow. K is the thermal conductivity of material considered and it changes depending on the material temperature. But, for many cases it is considered as

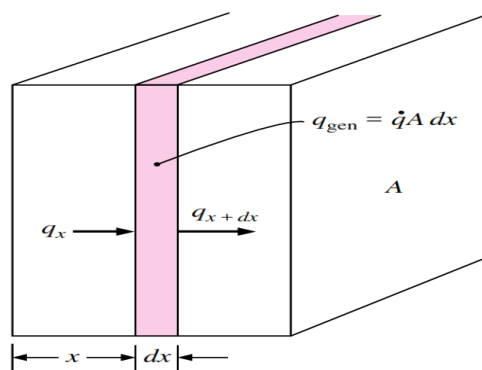


Figure 3.1 Heat conduction from the element (Holman,2019)

constant. The equation is called as Fourier's Law of Heat Conduction after the French mathematical physicist Joseph Fourier.

3.1.1.1. Thermal Conductivity

Defining the heat conductivity equation in previous section, thermal conductivity is the key variable as can be seen. By using the definition of heat conduction formulated in previous section, experiments have been done to determine the thermal conductivity of materials. Thermal conductivity is related to kinetic energy of the molecules. Basically, at high temperatures the kinetic energy of the molecules is higher i.e. molecules have higher velocities than that of molecules at lower temperatures. While molecules in a higher temperature region pass to the a region of lower temperature, they lose their kinetic energy to some extent by colliding each other and thus exchanging energy and momentum. In gas phase, the molecules move restlessly and randomly with no condition to temperature gradient existence. The molecules from higher temperature region to lower temperature region try to have equal temperature to be same as the final temperature of the system. During the process lower temperature region gains heat by conduction. Thermal conductivity depends on temperature differences between molecules and if molecules have higher velocity so they transfer heat faster compared to molecules moving at lower speed.

Physical description of the gases explains the behaviour of the liquids similarly. However, identifying the behaviour of liquid phase molecules are more difficult and the definition are more complex comparatively since they are closer to each other and molecular forces affects the energy exchange more as they collide. Thus, it cannot be excluded from thermal conductivity equations when liquids are in the scope. In solids, thermal energy transfer takes place via two ways. One way is by free electrons of a material with good thermal conductivity. The free electrons are exist in a lattice construction comprised of atoms and their electrons. These free electrons can both carry electric and thermal energy. Another way is lattice vibration.

Thermal conductivity expressed as $W/m^{\circ}C$ which is the definition of heat rate per meter per Celsius degree. Knowing that heat flux unit is shown as W/m^2 : heat flows the same direction with the unit area of a body.

3.1.2. Heat Transfer by Convection

Convection heat transfer is a major area of interest within the field of heat transfer. Therefore, the majority of the studies have been done focusing on convection heat transfer rather than conduction and radiation. Because of its unpredictable character and the variation of heat transfer significantly according to the shape of the surfaces, temperatures, flow rate, micro and nanoscale properties of fluids and so on. Convection heat transfer is expressed by three different flow forms: laminar, transient, turbulent. These forms determined by Reynolds Number.

Convection heat transfer is the way by which heat transferred through convection which is in fact a complex way of conduction taking place between a solid and liquid or gas phases placed adjacent and a temperature difference is exist as with conduction between solids. For example, a cooling speed of a metallic hot ball in air is higher when the wind speed is higher and the temperature is lower. But in the case of stationary air with no wind, it will cool slowly. This shows the convection is a type of conduction and the speed of the molecules are important factor and increasing the heat transfer.

Heat transfer by convective way can be expressed as

$$q = hA(T_w - T_\infty) \quad (3.3)$$

Where h is the convection heat transfer coefficient and A is the area of the surface which the convection occurs. Therefore, the surface can be an inner & outer side of a tube or a rectangular plate. In both cases heat can be transferred by convection when there exist temperature difference. The reason that T_w is expressed as wall temperature and T_∞ is the fluid temperature which is accepted as infinite, that is, the temperature of the liquid is not changing during the process in which heat transfer continuously happens until the wall increase of fall to the fluid temperature.

3.1.3. Heat Transfer by Radiation

Heat transfer can occur not only between the adjacent molecules. It can be seen between the distant molecules having temperature differences. Unlike the conduction and convection heat transfer in radiation heat transfer, heat is not carried by molecules between the two nodes which have different temperatures. Instead, there has to be an empty, vacuumed, region between the two temperature nodes.

Between these two temperature nodes the heat transferred by electromagnetic radiation, which depends on the material emissivity and absorbance.

Blackbody and grey body are the terms of the emissivity identities of the materials. A blackbody radiation is represented that a material emits whole radiation that it can radiate to the surroundings and the reason why a blackbody emissivity accepted as 1 as a factor in below equation.

$$q_{emitted} = \epsilon\sigma AT^4 \quad (3.4)$$

If we rearrange the above equation by substituting $\epsilon = 1$ it becomes,

$$q_{emitted} = \sigma AT^4 \quad (3.5)$$

Where σ is the Stephan-Boltzman constant and can be written as $5.67 \times 10^{-8} \text{ W/m}^2\text{K}^4$.

A is the surface of the body emitting and T is the temperature difference between bodies. If the surface area of the one body is a cover of another one, this shows the cover body absorbs all the emitted radiation from the body inside.

The general radiation heat transfer equation can be written as for all bodies, black or grey:

$$\frac{q_{net\ exchange}}{A} = F_{\epsilon} F_G A (T_1^4 - T_2^4) \quad (3.6)$$

Where F_{ϵ} is the emissivity of function and F_G is the view (shape) function of the emitting body, respectively.

3.1.4. Thermophysical Features of Nanofluids

Thermophysical properties of nanofluids which is used in this study are given in Table 3.2 in detail. Pramuanjaroenkij et.al (Pramuanjaroenkij et al., 2018) studied numerically heat transfer enhancement of nanofluids and expressed some equations for thermophysical properties of nanofluids.

The effective density of a nanofluid expressed as

$$\rho_{nf} = \phi\rho_p + (1 - \phi)\rho_f \quad (3.7)$$

Where ρ_p is the nanoparticles density and ρ_f is the base fluid density in which nanoparticles dispersed ϕ is the volumetric concentration percentage and can be calculated with the equation as follows

$$\phi = \frac{V_p}{V_p + V_f} \quad (3.8)$$

Where V_p is the nanoparticle volume and V_f is the base fluid volume and this equation for very low nanoparticles volume fractions is approximately equal to

$$\frac{V_p}{V_f} \quad (3.9)$$

Specific heat of the nanofluid can be written as

$$C_{p,nf} = \phi C_{p,np} + (1 - \phi) C_{p,bf} \quad (3.10)$$

Where nf, np and bf subscripts indicate nanofluid, nanoparticle and base fluid respectively.

Another well-known used in (Xuan & Roetzel, 2000) for specific heat of the nanofluid is

$$C_{p,nf} = \left[\frac{(\phi \rho_{nf} C_{p,np} + (1 - \phi) \rho_{bf} C_{p,bf})}{\rho_{nf}} \right] \quad (3.11)$$

Dynamic viscosity of the nanofluid significantly affects the nanofluid flow such as causing pressure drop and heat transfer. Various equations have been presented to define the dynamic viscosity of the nanofluids from the Einstein (Einstein, 1911) and his formula for nanofluid with spherical and very low volume percentage of nanoparticles is written

$$\mu_{nf} = (1 + 2.5\phi)\mu_{bf} \quad (3.12)$$

Where μ_{nf} and μ_f are the dynamic viscosity of the nanofluid and base fluid respectively. In this equation interaction between nanoparticles are ignored.

Another viscosity model developed by Brinkman (1952) expressed as

$$\mu_{nf} = \frac{1}{(1-\phi)^{2.5}} \mu_{bf} \quad (3.13)$$

Batchelor (1977) accepted the formula as

$$\mu_{nf} = (6.2\phi^2 + 2.5\phi + 1)\mu_{bf} \quad (3.14)$$

Maïga et al. (2004) wrote the dynamic viscosity equations as

$$\mu_{nf} = (123\phi^2 + 7.3\phi + 1)\mu_{nf} \quad (3.15)$$

Thermal conductivity has been seen as the main research of interest and many equations generated by researchers.

Maxwell (1873) was the first scientist who introduced the effective thermal conductivity of the nanofluids with spherical nanoparticles as

$$k_{nf} = \frac{k_p + 2k_{bf} + 2(k_p - k_{bf})\phi}{k_p + 2k_{bf} + (k_p - k_{bf})\phi} k_{bf} \quad (3.16)$$

This classical Maxwell model improved to decrease the error by considering the effect of Brownian motion of nanoparticles and written as:

$$k_{nf} = k_M + k_B \quad (3.17)$$

Where k_M the classical static Maxwell model is applied for solid-liquid mixtures and k_B is the thermal conductivity of Brownian model which is expressed as:

$$k_B = 5 \times 10^4 \beta_\beta \phi \rho_{bf} C_{p,bf} \sqrt{\frac{\kappa_B T}{\rho_p d_p}} f \quad (3.18)$$

Where

$$\beta_\beta = 0.0017(100\phi)^{-0.0841} \quad (3.19)$$

Finally a more precise model developed by Yu and Choi (2003). The equation does not ignore the monolayers covering the nanoparticles and written as

$$k_{nf} = \frac{k_p + 2k_{bf} + 2(k_p - k_{bf})(1 + \beta^3)\phi}{k_p + 2k_{bf} + (k_p - k_{bf})(1 + \beta^3)\phi} k_{bf} \quad (3.20)$$

3.2. Mathematical Model

Heat transfer equations were used in order to obtain a detailed mathematical model and calculate the efficiency of the flat-plate solar collector by using different nanofluids. In mathematical model, three main objectives were taken into consideration due to their great effects on efficiency of FPSC. Top heat loss coefficient, heat transfer coefficient of the working fluid, instantaneous efficiency of the FPSC. The mathematical modelling procedure in this thesis can be written as follows:

- Describing flat-plate solar collector dimensions
- Detailed description of the tube dimensions
- Investigation of the temperature nodes
- Energy balance equations in fin element
- Top heat loss coefficient of the collector
- Convection heat transfer coefficients of working fluids including nanofluids
- Efficiency of the flat-plate solar collector by calculating: collector flow factor, collector efficiency factor, collector heat removal factor, useful heat gain

A typical single glazed flat-plate solar collector can be seen in Figure 3.2.

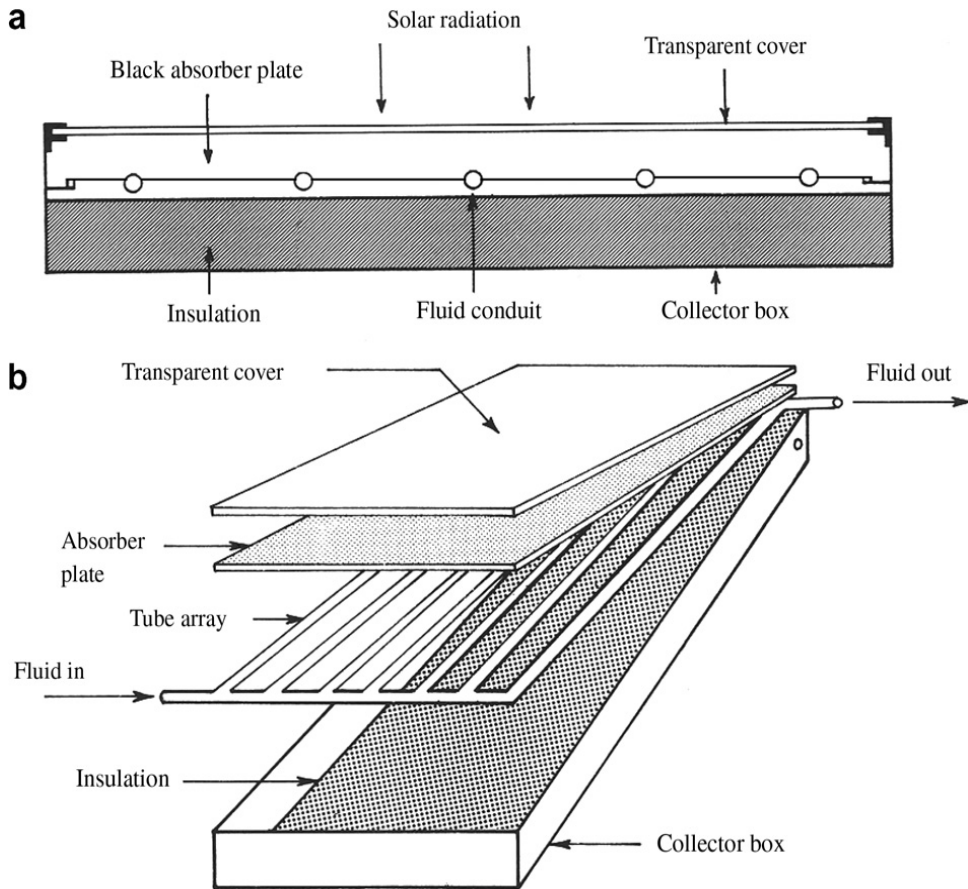


Figure 3.2 Components of FPSC: (a) cross-sectional view (b) isometric view (Sözen et al., 2008)

Over the course of the procedure applied in mathematical modelling contains some assumptions as follows:

- All parameters effecting performance is steady state.
- The design of the tubes are parallel and sheet attached with bond.
- The dimensions of headers can be neglected.
- Uniform flow due to the headers
- Absorbed solar energy by glass cover can be neglected.
- One dimensional heat flow exists through the cover
- Temperature drop because of the cover is ignored.
- There exists one dimensional heat flow through the back and edge insulations.

- The sky is accepted as blackbody and heat transfer as long wave radiation at the same temperature of sky.
- Temperature differences around tubes is negligible.
- Temperature nodes between flow direction and tubes are separately considered.
- The temperature of the environment are the same around the flat-plate collector. Thus, heat transfer through environment at the equivalent temperature.
- There is no shading of the absorber plate.
- Dust on the collector is neglected.

3.3. Heat Losses

3.3.1. Overall Heat Loss Coefficient

These sections cover the calculation of top heat loss coefficient of the flat-plate solar collector. To calculate it, absorber plate emittance and the space filled with air between cover and absorber plate were considered. A typical single glazed flat-plate solar collector with heat gains and losses can be seen in Figure 3.3.

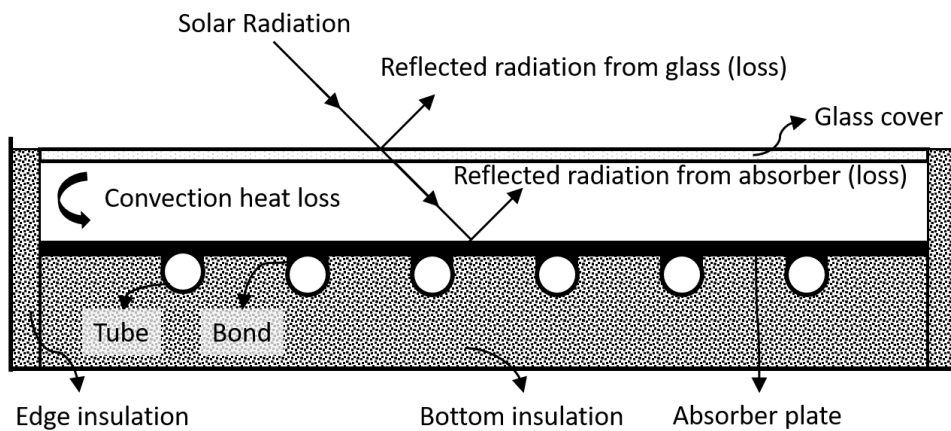


Figure 3.3 Heat losses from flat-plate solar collector in cross sectional view.

For determining the top heat loss coefficient of the flat-plate collector an iterative process is needed. Guessing both the absorber plate temperature and glass temperature and fixing the plate temperature during the process is applied in the procedure. Radiative heat transfer coefficient between from plate to glass and glass

to ambient then will be calculated by using these guessed values. It will be also used for evaluating the convective heat transfer coefficient together with those radiative heat transfer coefficients. All these heat transfer coefficients along with wind convection transfer coefficients are used to determine top heat transfer coefficient. In an iterative way, the results will then be returned and substituted into the related equations and real glass temperature is found according to guessed absorber plate temperature. The iteration is prolonged until the new value of glass temperature becomes as close to as glass temperature found in previous iteration in the loop. Ambient temperature is an important parameter here to create heat losses since the heat rate changes according to the temperature difference magnitude.

The calculation time can be very long due to lots of parameters and equations; thus, a computer program is written in Python 3.7 and used to shorten the time.

Heat transfer occurs between two different temperature nodes. After the collector absorbed solar radiation and heat losses to the surroundings take places due to temperature differences between the high collector temperature and the low ambient temperature. The collector can be imagined as a rectangular prism which is full and solid. So, assuming the collector like above description heat losses occurs from the top, considerably, edges and back. Thus, the total heat losses from the collector becomes,

$$U_L = U_t + U_b + U_e \quad (3.21)$$

Where U_t is the top heat loss coefficient and calculated for all temperature values according to simulation conditions and the graph presented in results section. U_b is the heat losses from the bottom of the collector and it can be expressed as,

$$U_b = \frac{k}{L} \quad (3.22)$$

And heat losses from the edges can be calculated from the following equation,

$$U_e = \frac{(UA)_e}{A_c} \quad (3.23)$$

Where A_e is the total rectangular areas of the edges of the solar collector while A_c depicts the collector area.

Top heat loss coefficient of the flat-plate collector is more complex and it will be explained in the further sections in detail.

3.3.2. Top Heat Loss Coefficient

Among the thermal losses from the flat-plate collector, the majority of the losses are from the top of the collector due to the reradiation from the absorber plate to the ambient and the heat losses by convection between plate to glass or glasses, if the collector has more than one glass covers such as double or triple glazed. Although, there exists losses from the edges or bottom of the collector. These are reduced mostly by insulation. The top of the flat-plate collector cannot be insulated due to the transparency requirements since the solar energy coming from this direction and should be absorbed at most. However, selective coatings are applied on top of collector.

Top heat loss coefficient of the flat-plate collector can be calculated by determining the components and thermal resistance network in terms of plates and covers. Temperature nodes then must be calculated. In this study single glazed flat-plate solar collector will be considered and top heat loss coefficient of the FPSC will be calculated by using iterative methods in Python programming language for broad temperature ranges of plate and glass accordingly.

A schematic drawing of cross-sectional view for a single-cover flat-plate solar collector shown in Figure 3.3.

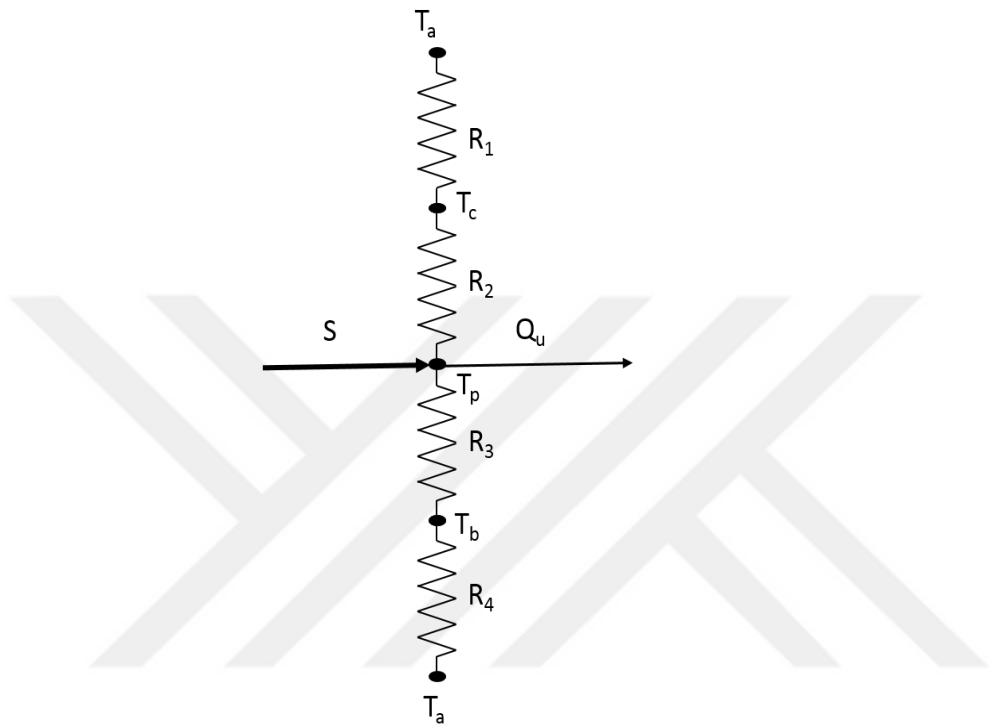


Figure 3.4 Thermal resistance network of single cover flat-plate solar collector with respect to resistances between plates.

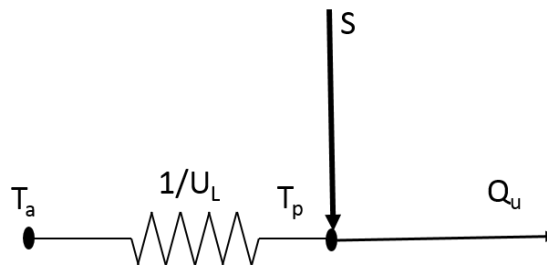


Figure 3.5 A brief overview of the thermal resistance network

Top heat loss according to the thermal resistance network becomes;

$$q_{top \text{ heat loss}} = h_{c,p-c}(T_p - T_c) + \frac{\sigma(T_p^4 - T_c^4)}{\left(\frac{1}{\epsilon_p}\right) + \left(\frac{1}{\epsilon_c}\right) - 1}$$

Where $h_{c,p-c}$ is the convection heat transfer coefficient between plate and cover. This equations can be simplified as follows

$$q_{top\ heat\ loss} = (h_{c,p-c} + h_{r,p-c})(T_p - T_c) \quad (3.24)$$

Heat transfer from the cover to the environment takes place by radiation and the sky temperature accepted as ambient temperature for calculation and so the resistance R_1 can be expressed as

$$R_1 = \frac{1}{h_w + h_{r,c-a}} \quad (3.25)$$

Where the $h_{r,p-c}$ is the convection heat transfer coefficient of the air between the plate and therefore cover and the definition of the resistance R_2 can be written as

$$R_2 = \frac{1}{h_{c,p-c} + h_{r,p-c}} \quad (3.26)$$

And radiation heat transfer coefficient can be written as

$$h_{r,c-a} = \frac{\sigma \epsilon_c (T_c + T_s)(T_c^2 + T_s^2)(T_c + T_s)}{T_c - T_a} \quad (3.27)$$

As the flat-plate collector having only one cover in this model, top heat loss coefficient can be written as

$$U_t = \frac{1}{R_1 + R_2} \quad (3.28)$$

The convective heat transfer coefficient for the wind expressed as

$$h_w = 5.7 + 3.8v \quad (3.29)$$

Convective heat transfer coefficient of the wind will be accepted as 10 W/m²K (Duffie et al., 2013) since the simulation will be tested according to laboratory conditions.

Collector heat losses should be reduced as much as possible to gain useful energy at maximum level. Top heat losses comprise of the majority of total heat losses from the flat-plate solar collector. Top heat loss can be defined as,

$$U_t = \left(\frac{1}{h_{c,p-c} + h_{r,p-c}} + \frac{1}{h_w + h_{r,c-a}} \right)^{-1} \quad (3.30)$$

Where radiative heat transfer coefficient of between plate and cover is

$$h_{r,p-c} = \frac{\sigma(T_p^2 + T_c^2)(T_p + T_c)}{\frac{1}{\epsilon_p} + \frac{1}{\epsilon_c} - 1} \quad (3.31)$$

Where T_p and T_c are the plate and glass cover temperatures respectively. Similarly, ϵ_p and ϵ_c shows the plate and cover emissivities respectively.

Between the collector and ambient there is a radiative heat transfer due to higher temperature of the collector compared to sky temperature. Therefore, radiative heat transfer coefficient from cover to sky can be expressed as follows

$$h_{r,c-a} = \epsilon_c \sigma (T_c^2 + T_s^2) (T_c + T_s) \quad (3.32)$$

And convective heat transfer coefficient between collector absorber plate and glass cover is found by the formula following

$$h_{c,p-c} = Nu \frac{k}{L} \quad (3.33)$$

Where Nusselt number is a dimensionless number and can be vary one scientist to another. Well-known variation of Nusselt number equations found in literature listed according to system design and related Reynolds number and forced or natural convection type accordingly. Nusselt number formula chosen for flat-plate solar collector simulated in this study can be written as

$$Nu = 1 + 1.44 \left(1 - \frac{1708}{Ra \cos \beta} \right) \left(1 - \frac{1708 \sin(1.8\beta)^{1.6}}{Ra \cos \beta} \right) + \left[\left(\frac{Ra \cos \beta}{5830} \right)^{\frac{1}{3}} - 1 \right] \quad (3.34)$$

Where β is the tilt angle of the collector and Rayleigh number then can be calculated after finding all parameters above that it includes as follows,

$$Ra = \frac{g(T_g - T_p)L^3 Pr}{T_{air} \nu^2} \quad (3.35)$$

Where Pr , ν can be obtained from the thermodynamic tables of air depending on its temperature, T_{air} . L is the glazing space in other words the distance between plates and cover which air placed. Glazing distance is less important for vacuumed flat-plate solar collectors than air filled ones comparatively. Pr refers to Prandtl number and ν is the kinematic viscosity which can be found by following equation

$$\nu = \frac{\mu}{\rho} \quad (3.36)$$

Applying the iteration among the equations the prediction of cover temperature and mean plate temperature is found from h_{rs} , h_{cp} and h_{rg} . After finding top loss heat transfer coefficient the T_g can be calculated from

$$T_g = T_p - \frac{U_T(T_p - T_a)}{h_{cp} + h_{rg}} \quad (3.37)$$

As long as the new T_g value found is less than the previous glass temperature the iteration is to be continued.

The process of calculating mean flat-plate temperature requires the overall heat transfer coefficient of the system. Iteration for this process is needed because the overall heat transfer coefficient of the flat-plate collector mainly depends on mean plate temperature. The mean plate temperature can be written as

$$T_p = T_{fm} + \frac{Q_u}{h_f \pi D_{in} L_p} \quad (3.38)$$

Where T_p is mean plate temperature and T_{fm} is the fluid mean temperature which is accepted as the average temperature found by averaging the sum of fluid temperature at the outlet and inlet pipe locations. L_p depicts the length of pipe inside the collector and D_{in} refers to the inner diameter of the pipe. As can be seen from the equation heat transfer coefficient of the fluid is important parameter and it can be concluded from the above equation that plate temperature less likely to increase when the heat transfer coefficient of the working fluid increases. This means heat is transferred to the heat transfer fluid rather than absorbed inside the absorber plate. Similarly, fluid mean temperature can be found by the following formula:

$$T_{fm} = T_i + \frac{Q_u}{U_L F_R A} \left[1 - \frac{F_R}{F'} \right] \quad (3.39)$$

Where F' is the collector efficiency factor and F_R is the heat removal factor. U_L is the total heat loss coefficient of the collector which is calculated above.

3.4. Heat transfer Coefficient of the Working Fluid

Heat transfer coefficient of the fluid used in the collector is of great importance since the heat absorption and transmission directly depends on this parameter as can be seen from the related equations. The main purpose of this study is to use different kind of working fluids and hence increase the efficiency of the flat-plate solar collector.

Heat transfer coefficient depends on many parameter of the fluid and the tube in which the fluid is flowing. The parameters effecting the heat transfer coefficient of the nanofluid explained in detail in the nanofluid preparation chapter. Flat plate solar collector was analysed by Duffie et al.(2013) in detail.

Heat transfer coefficient of the fluid flowing through the pipe of the collector can be formulated according to the control volume and dimensions shown in proceeding three figures.

$$S\Delta x - U_L\Delta x(T - T_a) + \left(-k\delta \left(\frac{dT}{dx}\right)\right)\Big|_x + \left(-k\delta \left(\frac{dT}{dx}\right)\right)\Big|_{x+\Delta x} = 0 \quad (3.40)$$

Where S is the solar energy absorbed by the control volume materials, U_L is he overall top heat loss coefficient of the collector, Δx is the length between initial and

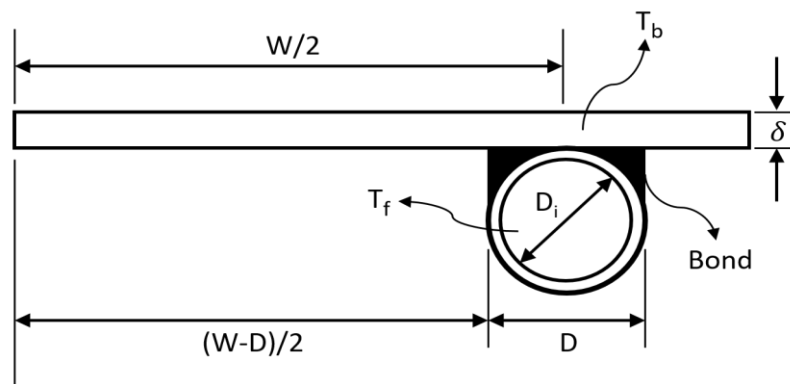


Figure 3.6 Tube and absorber plate dimensions

final points of flow, T is the final temperature, T_a is the ambient temperature, k is the thermal conductivity and δ is the thickness of the absorber sheet.

After dividing the above equation by Δx and calculating the limit while it is approaching zero, the formula becomes;

$$\frac{d^2T}{dx^2} = \frac{U_L}{k\delta} \left(T - T_a - \frac{S}{U_L} \right) \quad (3.41)$$

The equation above is a second order differential equation. Therefore, two boundary conditions are to be defined to solve it. The Figure 3.6 shows the pipe dimensions mirroring the half of it from the centre. The initial conditions in terms of temperature and distance depending on time is

$$\left. \frac{dT}{dx} \right|_{x=0} = 0 \quad (3.42)$$

And

$$T \Big|_{x=\frac{W-D}{2}} = T_b \quad (3.43)$$

To solve the problem easily two variables can be defined as

$$m = \sqrt{\frac{U_L}{k\delta}} \quad (3.44)$$

And

$$\xi = T - T_a - \frac{S}{U_L} \quad (3.45)$$

Now second order differential equation that we defined in the beginning can be written

$$\frac{d^2\xi}{dx^2} - m^2\xi = 0 \quad (3.46)$$

Expressing the boundary conditions for new formula

$$\left. \frac{d\xi}{dx} \right|_{x=0} = 0 \quad (3.47)$$

And

$$\xi \Big|_{x=\frac{w-D}{2}} = T_b - T_a - \frac{S}{U_L} \quad (3.48)$$

Finally, the general solution becomes

$$\xi = C_1 \sinh(mx) + C_2 \cosh(mx) \quad (3.49)$$

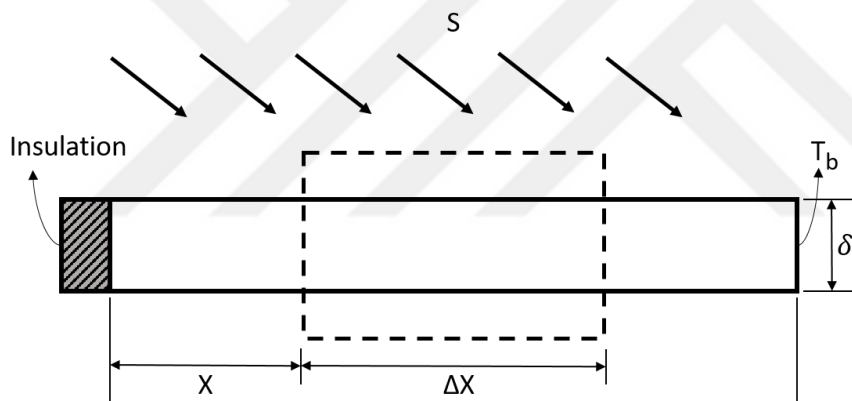


Figure 3.7 Energy balance in control volume of flow in pipe element

Boundary conditions should be substituted into general solution in order to determine the constants: C_1 and C_2 . Then the formula can be written as

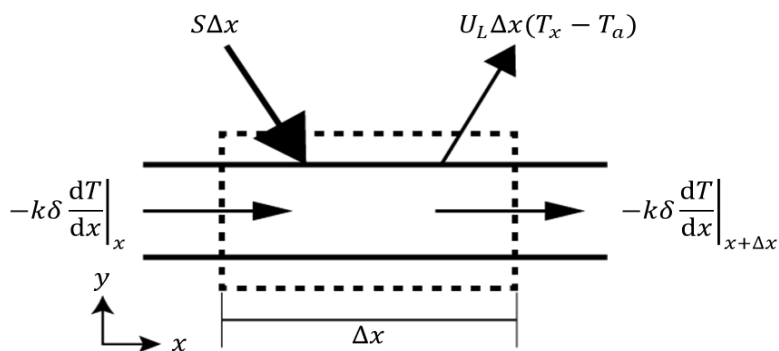


Figure 3.8 Energy balance of the control volume in the tube of the FPSC

$$\frac{T - T_a - \frac{S}{U_L}}{T_b - T_a - \frac{S}{U_L}} = \frac{\cosh(mx)}{\cosh\left[\frac{m(W-D)}{2}\right]} \quad (3.50)$$

Now conduction heat transfer formula can be used to define the energy transferred through the unit length of the pipe considering at the fin base:

$$q'_{fin} = -k\delta \left(\frac{dT}{dx}\right) \Big|_{x=\frac{W-D}{2}} = \left(\frac{k\delta m}{U_L}\right) [S - U_L(T_b - T_a)] \tanh\left(\frac{m(W-D)}{2}\right) \quad (3.51)$$

This equation considered for only one side of the tube; therefore, for both sides of the regarding schematic obtained energy can be expressed as

$$q'_{fin} = (W - D)[S - U_L(T_b - T_a)] \left[\frac{\tanh\left(\frac{m(W-D)}{2}\right)}{\frac{m(W-D)}{2}} \right] \quad (3.52)$$

Fin efficiency equation can be written here for rectangular flat fin as

$$F = \left[\frac{\tanh\left(\frac{m(W-D)}{2}\right)}{\frac{m(W-D)}{2}} \right] \quad (3.53)$$

Where W tubes spacing and D is the diameter of tube. Energy also obtained from the top of the tube as follows

$$q'_{tube} = D[S - U_L(T_b - T_a)] \quad (3.54)$$

Now the total useful heat gain from tube and fin can be written as

$$q'_u = [(W - D)F + D][S - U_L(T_b - T_a)] \quad (3.55)$$

Even a small effect but a factor can be considered here the bond connecting the tube to the absorber plate. Therefore, the transferred heat to the fluid can be expressed as below equation

$$q'_u = \frac{T_b - T_f}{\frac{1}{h_{fi}\pi D_i} + \frac{1}{C_b}} \quad (3.56)$$

Where h_{fi} is the fluid heat transfer coefficient (convection) and D_i is the inlet diameter of the tube and C_b is the bond conductance and can be found by the following equation

$$C_b = \frac{k_b b}{\gamma} \quad (3.57)$$

Where k_b is the thermal conductivity, b is the width and γ is the thickness of the bond respectively and usually this equation is ignored due to its least effect. The bond conductance as a parameter for calculating the efficiency of the flat plate solar collector simulation in this study accepted as constant and integer and can be seen in Table 3.1 Collector parameters

To sum up, collector efficiency factor can be expressed as

$$F' = \frac{\left(\frac{1}{U_L}\right)}{W \left[\left(\frac{1}{U_L(D + (W - D)F)}\right) + \left(\frac{1}{C_b}\right) + \left(\frac{1}{\pi D_i h_{fi}}\right) \right]} \quad (3.58)$$

Where h_{fi} is the heat transfer coefficient of the inlet working fluid and it can be calculated from the equations below

$$h_{fi} = \frac{Nuk}{D} \quad (3.59)$$

Where k is the thermal conductivity of the nanofluid, D is the diameter of tube inside and Nu is a dimensionless Nusselt Number which is to be determined.

Since it is a fluid flowing inside a circular tube of collector this becomes a convection heat transfer problem.

Initially, Reynolds Number must be calculated to determine whether the fluid flow is laminar, transient or turbulent

$$Re = \frac{\rho V D}{\mu} \quad (3.60)$$

And it also can be expressed as:

$$Re = \frac{V_{ave}D}{\alpha} \quad (3.61)$$

Where V_{ave} is the average velocity of the fluid inside the tubes of the collector and α is the thermal diffusivity and D is the diameter of the inside of the tube.

$$V_{ave} = \frac{\dot{m}\rho}{A_s} \quad (3.62)$$

Where ρ is the density of the fluid and \dot{m} is the mass flow rate of the fluid and A_s is the surface area of the inner side of the tube.

After finding the results, Reynolds number was seen lower than the critic number of 2300. Therefore, for this design and parameters the fluid flow is accepted as laminar and further calculations are made according to the flow character.

Second criteria is to taken into consideration is critic length for determining flow characteristic. Which is

$$L_{t,Laminar} \approx 0.05ReD \quad (3.63)$$

Making the calculation, the result shows that L_t is shorter than total length of pipe inside the collector so we can assume that the flow is thermally developing flow. Thus, Nusselt Number becomes;

$$Nu = 3.66 + \frac{0.065 \left(\frac{D}{L}\right) RePr}{1 + 0.44 \left[\left(\frac{D}{L}\right) RePr\right]^{\frac{2}{3}}} \quad (3.64)$$

Heat removal factor is an important parameter for determining the absorbed solar energy and heat loss and it can be found by following equation

$$F_R = \frac{\dot{m}C_p}{A_c U_L} \left[1 - \exp \left(- \left(\frac{A_c U_L F'}{\dot{m} C_p} \right) \right) \right] \quad (3.65)$$

It can be demonstrated by indicating absorbed solar radiation and ambient, fluid inlet and outlet temperatures as follows

$$F_R = \frac{\dot{m}C_p(T_{fo} - T_{fi})}{A_c(S - U_L(T_{fi} - T_a))} \quad (3.66)$$

Where S is the absorbed solar radiation, A_c is the collector surface area and constant, T_{fi} is the inlet fluid temperature, T_{fo} is the outlet fluid temperature of the collector, U_L is the overall heat loss coefficient, T_a is the ambient temperature, C_p is the specific heat capacity of the working fluid and \dot{m} is the mass flow rate of the fluid inside the collector pipes, respectively.

Heat removal factor is also equal to that of collector flow factor multiplied by collector efficiency factor.

$$F'F'' = F_R \quad (3.67)$$

Collector flow factor varies in the range $0 < F'' < 1$ as can be seen in Figure 3.9.

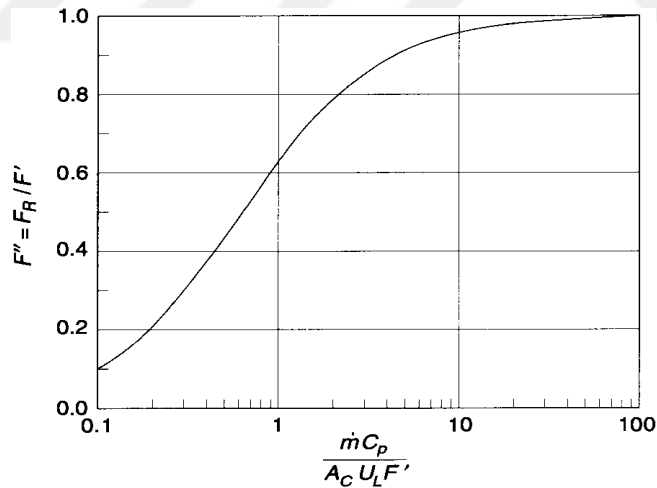


Figure 3.9 Collector flow factor with dimensionless collector capacitance rate (Duffie, et.al, 2013)

3.5. Useful Heat Gain and Thermal Efficiency

The heat loss from the collector occur when its temperature becoming higher than the ambient temperature after receiving heat from sun and thus the formulation can be written as ,

$$Q_o = U_L A(T_p - T_a) \quad (3.68)$$

Hence, the useful heat gain of the collector can be calculated by subtracting these losses to the ambient. Useful heat gain now can be expressed as:

$$Q_u = Q_i - Q_o \quad (3.69)$$

The definition can also be written with respect to hourly solar radiation as

$$Q_u = A[IR(\tau\alpha)_s - U_L(T_p - T_a)] \quad (3.70)$$

Useful thermal energy gain from the absorber can be found by subtracting the total heat loss from the collector from the possible maximum energy gain from solar radiation coming to the collector.

$$Q_u = F_R A_c (S - U_L(T_i - T_a)) \quad (3.71)$$

Where absorbed solar radiation by collector can be expressed as

$$S = I_b R_b (\tau\alpha)_b + I_d (\tau\alpha)_d \left(\frac{1 + \cos\beta}{2} \right) + \rho_g I (\tau\alpha)_g \left(\frac{1 - \cos\beta}{2} \right) \quad (3.71)$$

Where b, d, g subscripts show beam, diffuse and ground solar radiations, respectively. The tilt angle of the solar collector is depicted as β . The above equation defined for the any location on earth exposed to all ambient conditions including all solar direct and indirect incidents. However, in simulation, reflected radiation and diffuse radiation from the environment were neglected and only direct incident solar radiation was taken into consideration.

Average transmittance-absorptance product is roughly equal to that of beam transmittance-absorptance product and can be calculated as

$$\tau\alpha_{ave} \approx 0.96(\tau\alpha)_b \quad (3.72)$$

Thus, replacing the product in the above equation

$$Q_u = A_c F_R (\tau\alpha)_{ave} G_T - F_R U_L A_c (T_i - T_a) \quad (3.73)$$

Rearranging the equation useful energy gain can be simplified as follows

$$Q_u = [A_c F_R [(\tau\alpha)_{ave} G_T - U_L(T_i - T_a)]] \quad (3.74)$$

Where A_c is the collector gross area, F_R is heat removal factor, G_T is total irradiation reaching the surface of the collector as W/m^2 , U_L is the total heat loss coefficient, T_i is the fluid inlet temperature and T_a is the ambient temperature. This equation will be used in the code when determining useful heat gain in modelling of plate solar collector.

Efficiency of the thermal systems can be complex. But in literature and approaches for engineering purposes united for simplified formulations used for both experimental and theoretical tests. Instantaneous efficiency of the flat-plate solar collector therefore, formulated as follows,

$$\eta = \frac{Q_u}{A_c G_T} \quad (3.75)$$

Where G_T can be replaced by I or H according to hourly or daily solar radiation data. If the heat removal factor is to be taken into account and outlet fluid temperature is omitted from the equation the efficiency of the flat-plate collector becomes

$$\eta = \left[F_R (\tau\alpha)_{ave} - F_R U_L \left(\frac{T_i - T_a}{G_T} \right) \right] \quad (3.76)$$

Where collector F_R is heat removal factor, $\tau\alpha_{ave}$ is transmittance-absorptance product, U_L is overall heat transfer coefficient, T_i is the inlet fluid temperature and T_a is the ambient temperature, respectively.

3.6. Modelling Simulation

There are many experimental investigations in order to calculate the efficiency of the flat-plate solar collector with or without nanofluids. However, there are certain drawbacks associated with the use of experimental method. A major problem with the experimental method is that the all parameters affecting the results are not under control and not stable. Some parameters are kept under control and investigated parameters are altered. The stability of the system is another major problem and this causes a great gap among the results obtained from different experiments. Because, the stability of the controlled parameters is not totally the same during the experiment. Therefore, there exist another approach to evaluate a system. The simulation method is one of the more practical ways of determining the efficiency of the collector in various conditions. Simulation model is actually combined

theoretical model derived from the experimental results and it is comprising of the any parameters given by equations and conditions. For flat-plate solar collector these conditions and parameters: temperature changes of any temperature nodes, working fluid, wind, shading, dust, mass flow rate, sizes of components etc.

The simulation developed in this study to obtain performance of the flat-plate solar collector filled with different nanofluids and water. The simulation parameters accepted according to a solar collector which is in laboratory conditions and no dust effects or reflected radiation taken into consideration. Some important parameters and the mathematical equations used in the simulation will be identified in this subsection. The simulation parameters for single glazed flat-plate solar collector can be seen in Table 3.1.

Table 3.1 Collector parameters

Collector Parameters	Symbol	Value	Unit
Tube Spacing	W	0.025	m
Tube Diameter	D	0.01	m
Plate Thickness	δ	0.001	m
Plate thermal conductivity	k	0.2	W/(m°C)
Incident solar radiation	G_T	800	W/m ²
Bond Conductance	C_b	345	W/(m°C)
Ambient temperature	T_a	20	°C
Absorptance of the absorber sheet	α	1	
Transmittance of the glass	τ	0.84	
Glazing Space	L	0.025	m
Glass Emissivity	ϵ_g	0.88	
Absorber plate emissivity	ϵ_p	0.95	
Tilt Angle	β	45	degree(°)
Collector surface area	A_s	1	m ²

Mass flow rate refers to the volumetric flow rate of the working fluid flowing through the pipes of the collector where density of the fluid is not constant and mass flow rate changes accordingly. But, ASHRAE 93-2003 standards offer an experimental test conditions in which mass flow rate of the fluid can be measured as 0.02 kg/s. Thus, the mass flow rate of the all working fluid tested in the simulation accepted as 0.02 kg/s and constant during the process.

Ambient temperature is environment temperature surrounding the whole system and its components accepted as constant and the initial fluid temperature as 20 °C .

Viscosity refers to dynamic viscosity of the fluids and it was accepted as the initial viscosities of all fluids for whole processes. But the air viscosity for calculating top heat loss coefficient was taken into consideration thanks to the valid information regarding the air thermal properties in literature. Thus, more precise results were obtained for top heat loss coefficient after conducting the iterative process by using Python code can be seen in Appendix 1 and 2.

3.6.1. Model of the Top Heat Loss Coefficient

The program `topheatloscoefficient.py` can be found in Appendix () is used to calculate top heat loss coefficient of the collector as a function of absorber plate temperature. The input parameters below should be entered to the program:

- Solar irradiance, G_t
- Glass temperature guess value
- Plate temperature
- Ambient temperature

After entered these parameters, the program was run and the actual glass temperature and top heat loss coefficient of the single glazed flat-plate solar collector was found. The simulation code then modified to calculate actual glass temperature and top heat loss coefficient of the collector in the absorber plate temperature range of 30-100 °C. Finally, collector top heat loss coefficient for given range of absorber plate temperature was calculated. The result can be seen in Figure 4.1. According to this graph the average collector top heat loss coefficient for the simulation temperature range was found and accepted as constant.

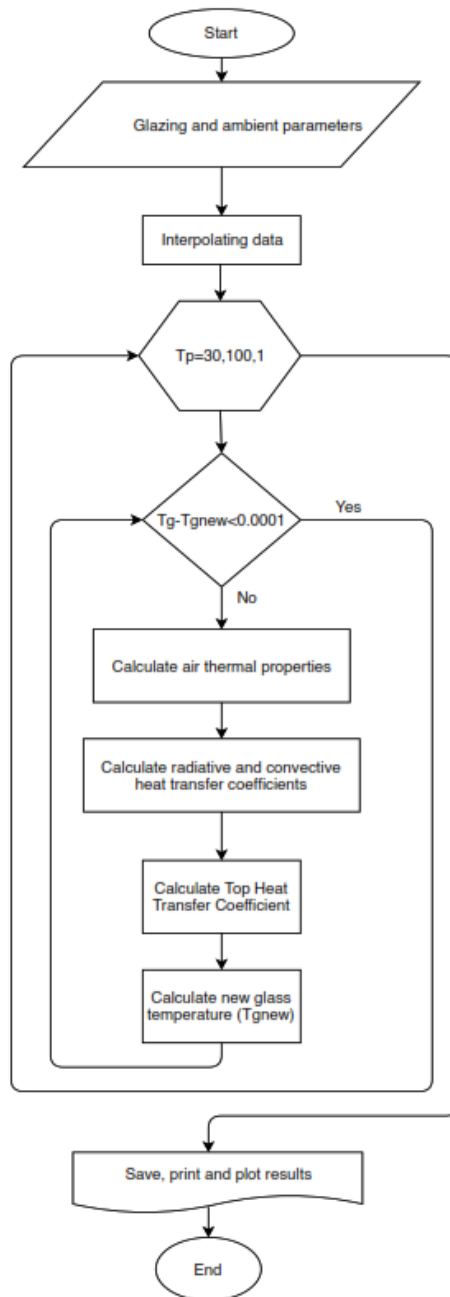


Figure 3.10 Flowchart of top heat loss coefficient program

A flowchart of the program, which can be seen in Figure 3.10, written for calculation of top heat loss coefficient of the flat-plate solar collector at the absorber temperature which is ranging from 30 to 100 °C.

3.6.2. Convection Heat Transfer of the fluid

Heat transfer coefficients of the nanofluids and water were modelled by using the related equations explained in mathematical model section. According to those equations, a flat-plate solar collector considered having parameters given in the table and working flow parameters were also calculated accordingly. The parameters below should be entered to the program in order to the obtain results.

- Tube diameter and length
- Density of the fluid
- Thermal conductivity of the fluid
- Dynamic viscosity
- Prandtl number
- Mass flow rate

Finally, the simulation will give the results listed below:

- Inner surface area of the pipe
- Average fluid velocity
- Reynolds Number
- Nusselt Number
- Convection heat transfer coefficient of the fluid

3.6.3. Efficiency Modelling

Instantaneous efficiency of the flat-plate solar collector were modelled according to the mathematical modelling of efficiency section. Some parameters needed to calculate efficiency of the flat-plate collector were found in top heat loss coefficient program and convection heat transfer coefficient program of the working fluid. So as to see the results numerically and also scattered version of a graph the parameters below should be entered

- Ambient temperature
- Transmittance and absorptance of the plate

- Solar radiation
- Collector area
- Density of the fluid
- Mass flow rate
- Tube spacing
- Tube diameter
- Fluid inlet diameter
- Heat transfer coefficient of the fluid
- Thermal conductivity of the bottom insulation
- Thickness of the bottom insulation
- Absorber plate thickness
- Top heat loss coefficient
- Heat loss coefficient of the edges

After running the simulation program, the results obtained will be:

- Fin efficiency
- Collector efficiency factor
- Heat removal factor
- Maximum possible useful heat gain
- Instantaneous thermal efficiency of the collector
- Reduced temperature parameter
- Inlet and outlet temperatures of the working fluid

3.7. Experiment Materials

In this study, simulation includes 5 different fluids. Water used as a conventional working fluid. The other four various nanofluids consists of two different nanoparticles with two different volume concentration. Nanoparticles used in this experiment are Al_2O_3 and Cu dispersed in water as a base fluid with 1% and 5% volume fractions. Both nanoparticles suspended in base fluid with the same volume fractions in order to compare both volume fraction and nanoparticle effects on thermal properties of nanofluid. Table 3.2 shows the thermal properties of water and nanoparticles and nanofluids which include these nanoparticles with different volume ratios. These nanofluids was used in the simulation and other required thermal properties such as Prandtl Number (Pr), thermal expansion coefficient (β) etc. were found by using these parameters and related equations.

Table 3.2 Thermal properties of nanofluids(Yurddaş, 2013)

	ρ (kg/m ³)	Cp (J/kgK)	k (W/mK)	μ (kg/ms)
Water	997.78	4076.4	0.60475	0.0009772
Al₂O₃	3970.8933	765	40	
Cu	8933	385	401	
Φ (%)	ρ (kg/m ³)	Cp (J/kgK)	k (W/mK)	μ (kg/ms)
1% Al₂O₃	1027.5022	3948.4562	0.62226	0.0010021
1% Cu	1077.1322	3770.2605	0.62299	0.0010021
5% Al₂O₃	1146.391	3503.0242	0.69582	0.0011109
5% Cu	1394.541	2894.1014	0.69978	0.0011109

Water as a reference fluid is also used and indicated for better comparison since it is well known working fluid in flat-plate solar collectors. As can be seen from the table that shows the nanofluids used in this study, increasing the nanoparticles concentration in base fluids result in specific heat capacity decrement but thermal conductivity and density increment. However, the viscosity is not depending on the particle material and it only depends on the volumetric concentration of the nanoparticles and viscosity increases with increase in particle concentration in base fluids. It also can be seen from the table than nanofluids which include nanoparticles having higher thermal conductivity are of higher thermal conductivity than that of nanofluids which have nanoparticles with lower thermal conductivity.

4. RESULTS AND DISCUSSION

4.1. Top heat losses

Although the density of the nanofluids and water used in the simulation accepted as the density at the initial state, air density alteration according to temperature taken into account while finding the top heat loss coefficient of the collector.

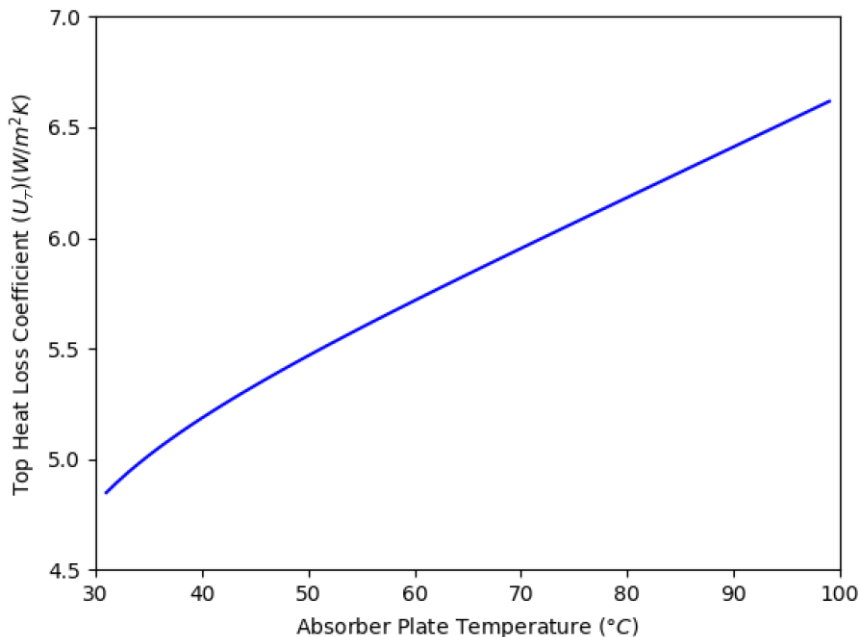


Figure 4.1 Top heat loss coefficient of the collector with absorber plate temperature

The line graph in Figure 4.1 illustrates changes in the top heat loss coefficient during the absorber plate temperature increase from 30 to 100 $^{\circ}C$ and measured in W/m^2K . It can be seen from the figure that the top heat loss coefficient of the flat-plate solar collector increases with increase in absorber plate temperature. It is to be mentioned that the graph is a curve and after around 55 $^{\circ}C$ and it is a linear function of temperature. Therefore, the top heat loss coefficient can be modelled and more precise results can be obtained from the fitted functions over the graph after some degrees but for the range of 30-50 $^{\circ}C$ top heat loss coefficient has a trend that is concave down.

4.2. Fluid Inlet and Outlet Temperatures

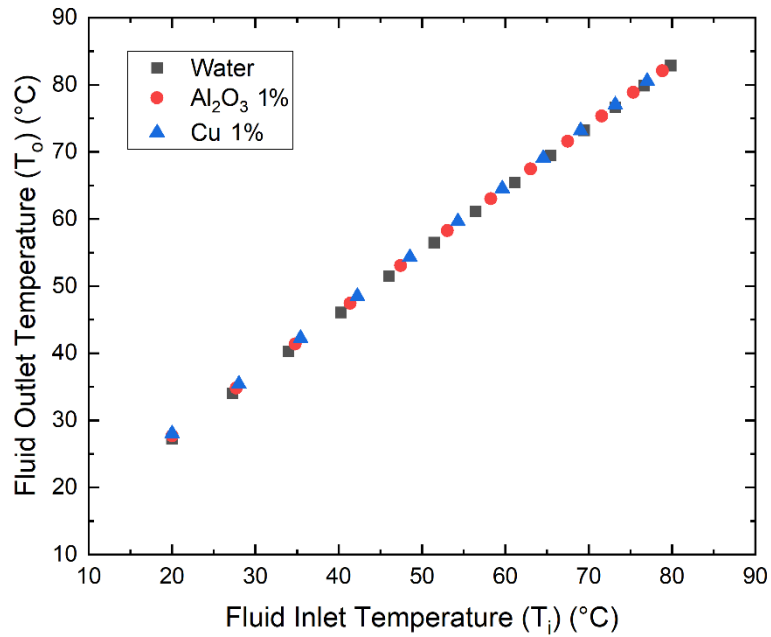


Figure 4.2 Collector outlet temperatures of Water, Al_2O_3 1% and Cu 1% with their inlet temperatures.

The scattered data in the Figure 4.2 demonstrates fluid outlet temperatures as a function of inlet temperatures of the collector in terms of three different fluids. Nanofluids shown in the figure have 1% volume fraction. The results show that outlet temperature of Al_2O_3 nanofluid with 1% volume fraction increases with increase in fluid inlet temperature. Similarly, outlet temperature of nanofluid which has Cu nanoparticle with a volume concentration of 1% was also increased with increase in inlet temperature. Overall, it can be seen from the figure that fluid inlet temperatures of the all working fluids inside the collector is initially the same. However, outlet temperatures vary from one fluid to another. Outlet temperature of Al_2O_3 nanofluid with 1% volume concentration increased more than that of water. Likewise, the outlet temperature of the Cu nanofluid having 1% nanoparticle volume fraction was increased more than both water and Al_2O_3 with 1% volume fraction. This shows the thermal properties of nanofluids affects the outlet temperature of the collector thus enhancing the overall efficiency.

Simulation program was run by limiting the outlet temperature 80 °C and equalized outlet temperatures to inlet temperatures after the initial temperatures as it is accepted as no heat loss from the working fluid while flowing through the pipes from the outlet to the inlet of the collector. From the figure, it can be observed that and all fluids reached this level by spending different time durations. Cu nanofluid with 1% volume fraction was the first one whose temperature surpassed the 80 °C and became higher. Second fluid was nanofluid having 1% Al₂O₃ nanoparticles. The conventional fluid which is pure water spent the most time required to reach the temperature level of 80 °C. It is obvious that the outlet temperature increment for each cycle is decreasing due to the useful heat gain decrement.

In previous studies, inlet and outlet temperatures of flat-plate solar collector were examined. The results show that collector inlet temperature increases with increase in outlet temperature and when the mean plate temperature and the ambient temperature of the flat-plate solar collector accepted as constant during the process. The heat losses from the working fluid flowing from the collector outlet to the inlet of the collector are neglected since the carrier tubes connected to inlet and outlet pipes accepted as super insulated therefore not allowing the heat transfer through them.

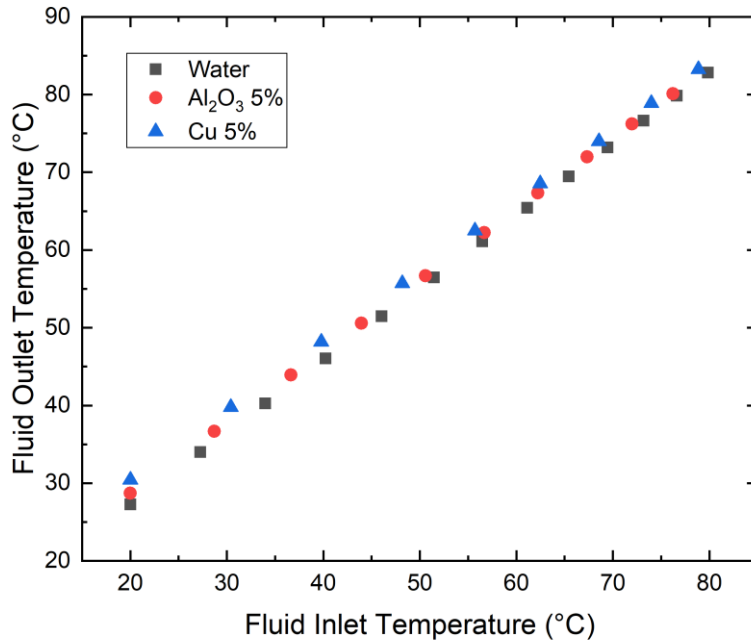


Figure 4.3 Collector outlet temperatures of Water, Al₂O₃ 5% and Cu 5% with their inlet temperatures.

The Figure 4.3 illustrates fluid outlet temperatures with inlet temperatures of the collector including three different fluids. Similar to previous figure, all fluid outlet temperatures increased during the simulation due to the fact that inlet temperatures increased.

In comparison to the Figure 4.2 the outlet temperatures of fluids are higher from the flat-plate solar collector due the fact that the specific heat capacity of the nanofluids are lower when the nanoparticle volume concentration is higher. This shows that not only thermal conductivity of the nanofluids affects the useful heat gain and outlet temperatures of the working fluids accordingly. So, it can be concluded that when the specific heat capacity of the working fluids is lesser the useful heat gain is less but the outlet temperature of working fluids is therefore higher.

4.3. Useful Heat Gain

From the figure it can be concluded that the top heat loss coefficient is not a linear function of the absorber plate temperature. The top heat loss coefficient as a function of absorber plate is in increasing rate of change between the 30 °C and 50 °C and decreasing and curve is concave down and after 50 °C the function is more linear until 100 °C.

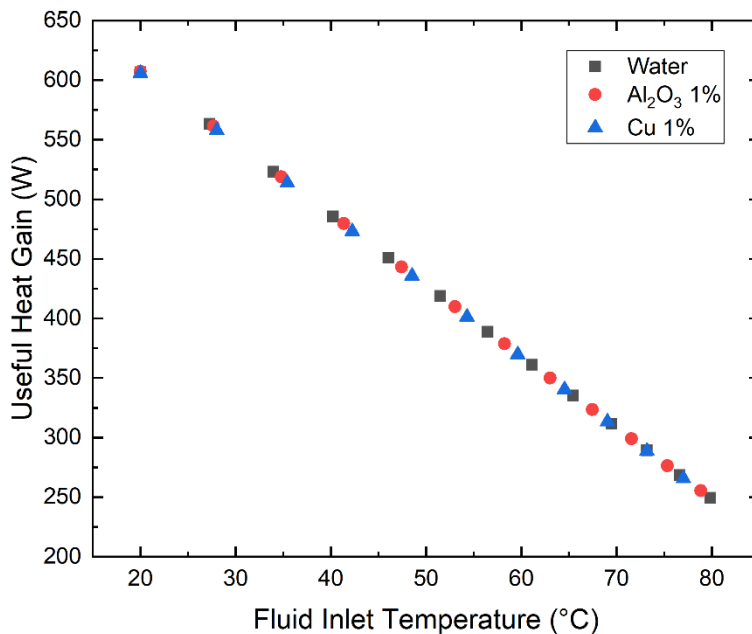


Figure 4.4 Useful heat gain of the collector with fluid inlet temperature using three different working fluids: Water, Al₂O₃ 1% and Cu 1%.

The Figure 4.4 shows two different nanofluids with the same volume ratio of 1 percent together with pure water and their useful heat gains as a function of fluid inlet temperatures. As can be seen from the graph that useful heat decreases while fluid inlet temperature increases. Maximum useful heat gain of the collector for any fluid reached when the fluid inlet temperature is at lowest. Likewise, the minimum useful heat gain is obtained when the temperatures of the fluids are at the highest value. By comparing the nanofluids and water, it can be observed that owing to the fact that Cu nanofluid with 1% volume ratio shows faster temperature increment

than other fluids since it has the least useful heat gain in each cycle and Al_2O_3 nanofluid is following it in terms of useful heat gain. Water, however, obtains useful heat most because having lowest temperature increase in each period.

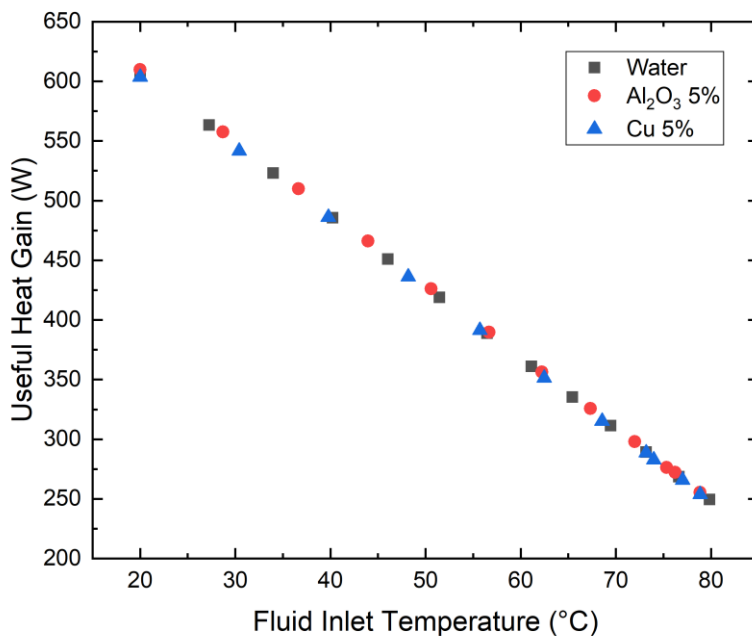


Figure 4.5 Useful heat gain of the collector with fluid inlet temperature using three different working fluids: Water, Al_2O_3 5% and Cu 5%.

The Figure 4.5 demonstrates the nanofluids with 5% volume concentration. It can be seen from the figure that it is similar to the Figure 4.4 but in this case the nanofluid Cu with 5% volume fraction reached higher fluid inlet temperature degrees than Cu with 1% volume concentration. It also surpassed the Al_2O_3 nanofluid with 1% volume fraction. In terms of useful heat gain, at the beginning of the simulation with the same fluid inlet temperature of 20 °C all working fluids have useful heat gains around 600 W but Al_2O_3 nanofluid with 5 percent volume concentration shows highest useful heat gain because of the fact that nanofluids' thermal properties.

4.4. Efficiency

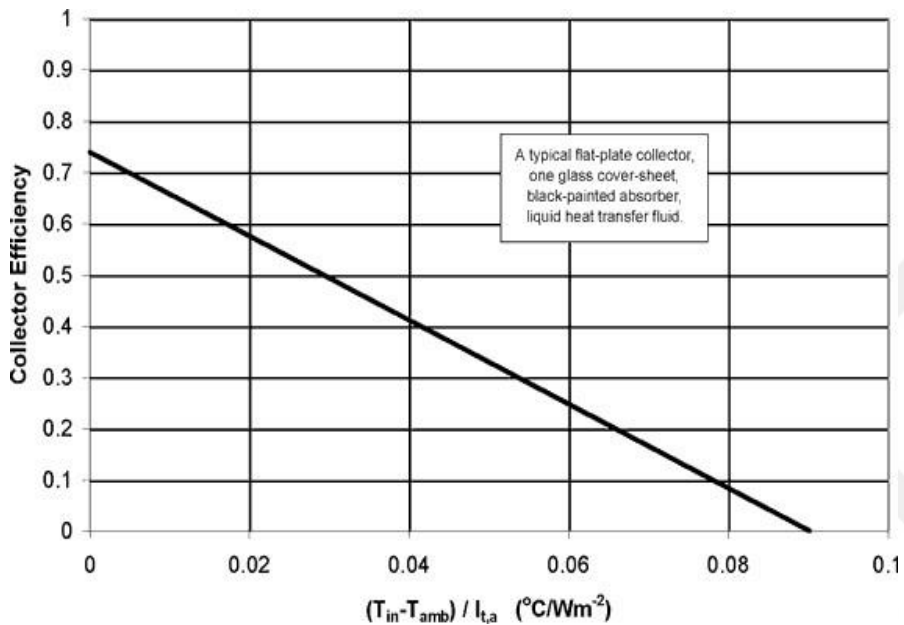


Figure 4.6 Efficiency of a common single glazed flat-plate solar collector (Struckmann, 2008)

The graph above shows the efficiency of the single glazed flat-plate collector tested. The equations written for simulation are also based on the standards in ASHRAE 93-2003. This standard is widely used around the world and trusted. As seen in the Figure 4.6, the efficiency of FPSC decreases linearly with an unchanged slope while temperature gap between ambient and fluid inlet temperature are increases. Obtained results from the simulation for the water in this study are in good agreement with the results of the standards. Based on that, various nanofluids were tested in the simulation.

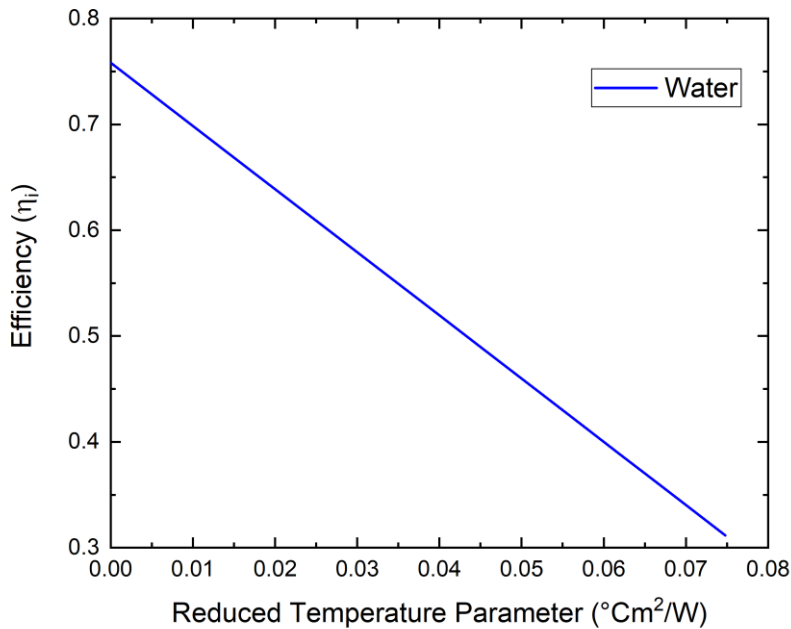


Figure 4.7 Efficiency of flat-plate collector using water with reduced temperature parameter

The line graph above shows the efficiency of the flat-plate solar collector as a function of reduced temperature parameter. Water as a conventional working fluid and a reference data were chosen in order to compare with nanofluids. The function of linear line graph has a negative slope of $F_R U_L$ product and as it can be seen that it is not changing during the simulation. As can be seen from the figure that the efficiency of the collector decreases with increase in reduced temperature parameter. It is apparent from the unit of reduced temperature parameter that increase in temperature of the inlet fluid of the water result in decrease in the efficiency of the collector. When the inlet temperature of the working fluid is equal to the ambient temperature, the efficiency of the flat-plate solar collector is maximum since there is no heat loss to the environment from the collector. During the simulation the transmittance-absorptance product ($\tau\alpha$) remained constant. Similarly, as it was accepted that overall heat loss coefficient is constant and similarly no change in the $F_R U_L$ product was observed.

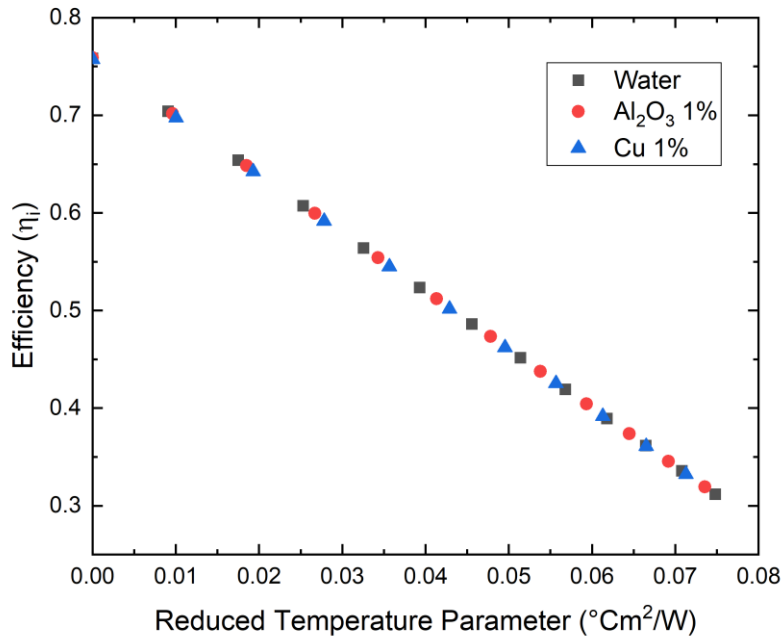


Figure 4.8 Efficiency of flat-plate collectors using Water, Al₂O₃ 1% and Cu 1% with reduced temperature parameter.

The figure above shows the efficiency of the flat-plate collector by using three different working fluid. Of fluids used, two are different nanofluids with 1% volume fraction. All working fluids show their highest thermal efficiencies when reduced temperature parameter is zero which means ambient temperature is equal to the fluid inlet temperature. Likewise, while reduced temperature parameter increases efficiency of the flat-plate solar collector decreases. However, having 1% volume fractions of Cu and Al₂O₃ nanofluids show higher efficiencies than water. Similarly, Cu nanofluid with 1% volume fraction shows the highest efficiency.

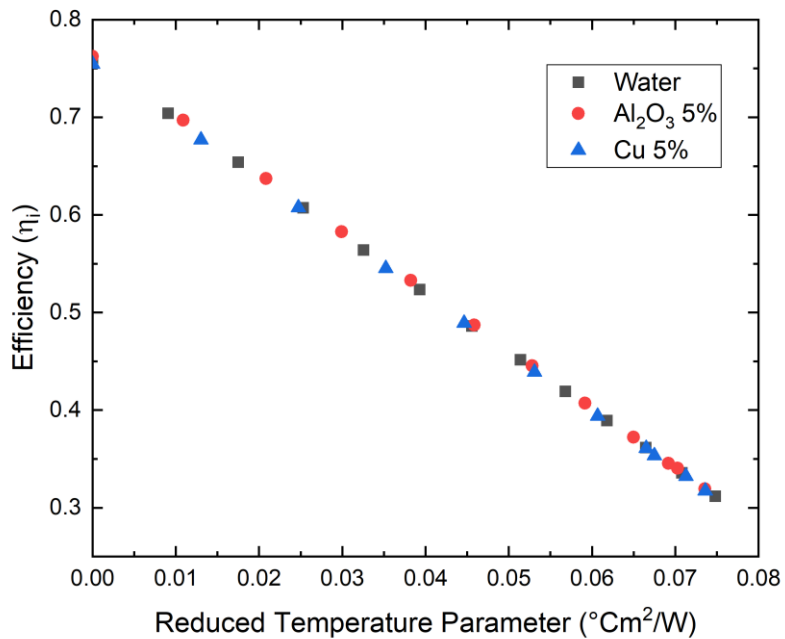


Figure 4.9 Instantaneous efficiency of the flat-plate solar collector with water, 5% Al_2O_3 and 5% Cu.

The graph above shows nanofluids with 5% volume concentrations and water and their effects on the instantaneous efficiencies of flat-plate solar collector with reduced temperature parameter. Comparing the previous figure that contains nanofluids with 1% volume fractions, the nanofluids with 5% nanoparticle volume fractions show better thermal conductivity and thus enhancing the efficiency of the flat-plate collector. Since it can be seen from the figure that the gap between scattered dots belongs to the three different working fluids are higher than that of previous figure. This shows that nanofluids with higher volume fractions transfer the heat better and reaches higher temperatures in a particular period than nanofluids with less nanoparticle volume fractions.

5. CONCLUSIONS

The aim of this study is to investigate the efficiency of the flat-plate collector by using various nanofluids with different volume fractions and water as a reference sample and base fluid. After reviewing the literature for flat-plate solar collectors filled with various nanofluids. A simulation program was then written in python according to detailed mathematical model and run for Al_2O_3 and Cu nanofluids with both 1% and 5% volume concentrations together with pure water. Conclusions from the results generated from the simulation can be written as follows:

- The nanofluid thermal conductivity increases with increase in particle volume fractions.
- Specific heat capacity of the nanofluids decreases with increase in nanoparticle volume concentration.
- Density of the nanofluids enhanced with increase in nanoparticle concentration and affected the heat transfer coefficient of the nanofluids. Therefore, it also affected the heat transfer and efficiency of the flat-plate solar collector.
- Collector heat removal factor and absorptance-transmittance products remained constant during the simulation. The negative (-) slope $F_R(U_L)$ also was also remained unchanged and its intercept with efficiency axis shows the maximum theoretical efficiency of the flat-plate solar collector. The slopes of efficiency lines with respect to the reduced temperature parameters were almost the same for all working fluids.
- Viscosity changes during the process owing to temperature change were taken into account when calculating top heat loss coefficient of the collector. However, for nanofluids viscosity was accepted as constant at the initial state of the process due to the lack of information about viscosity alteration due to temperature change of the given nanofluids in literature. Therefore, the viscosity of the nanofluid was not changed during the simulation. The related viscosity equations in literature could be used for calculating and considering the viscosity of nanofluids but theoretically the results of the nanofluids so far have not been matched. Since using these equations were not accepted as a proper method in this study. But for more precise results the viscosity changes of the nanofluids according to their temperature can be considered in further studies either using theoretical

equations for viscosity of nanofluids or empirical functions. The best result could be measuring viscosity of the sample nanofluid for each temperature during the process.

- Enhancement of the efficiency of the flat-plate collector by using nanofluids was observed.

It is important to indicate that the methodology used in this study has many uncertainties and assumptions. Every assumption or theoretical equations were scientifically explained and cited. The main focus was to build a complete mathematical model to express the efficiency of the flat-plate collector by using different nanofluids and thus three different programs were written and chained each other. At the end a simple and single ready to use program could be run to obtain reliable results.

Over the course of the modelling process many problems took place that could not be indicated or involved in this study and therefore further studies are required.

This study provides a comprehensive knowledge about flat-plate solar collector efficiency calculations with mathematical model and programming. The top heat loss coefficient especially examined in detail. The study also reveals the effects of nanofluids as novel working fluids in FPSCs. The results and codes of this study might contribute to researchers or engineers to assess the components or the working fluids of FPSCs in terms of their properties in the future and to take further decisions. A user interface can also be developed to use the program more efficiently.

REFERENCES

- Akbari, O.A., Afrouzi, H.H., Marzban, A., Toghraie, D., Malekzade, H. & Arabbour, A. 2017. Investigation of volume fraction of nanoparticles effect and aspect ratio of the twisted tape in the tube. *Journal of Thermal Analysis and Calorimetry*, 129(3): 1911–1922.
- Batchelor, G.K. 1977. The effect of Brownian motion on the bulk stress in a suspension of spherical particles. *Journal of Fluid Mechanics*, 83(1): 97–117.
- Brinkman, H. 1952. The viscosity of concentrated suspensions and solutions. *The Journal of Chemical Physics*, 20(4): 571–571.
- Challoner, A. & Powell, R. 1956. Thermal conductivities of liquids: new determinations for seven liquids and appraisal of existing values. *Proceedings of the Royal Society of London. Series A. Mathematical and Physical Sciences*, 238(1212): 90–106.
- Choi, S.U.S. & Eastman, J.A. 1995. Enhancing thermal conductivity of fluids with nanoparticles. : 9.
- Das, P.K. 2017. A review based on the effect and mechanism of thermal conductivity of normal nanofluids and hybrid nanofluids. *Journal of Molecular Liquids*, 240: 420–446.
- Das, P.K., Islam, N., Santra, A.K. & Ganguly, R. 2017. Experimental investigation of thermophysical properties of Al₂O₃–water nanofluid: Role of surfactants. *Journal of Molecular Liquids*, 237: 304–312.
- Das, S.K., Putra, N. & Roetzel, W. 2003. Pool boiling characteristics of nano-fluids. *International journal of heat and mass transfer*, 46(5): 851–862.
- Duffie, J.A., Beckman, W.A. & Worek, W. 2013. *Solar engineering of thermal processes*. 4th ed. Wiley Online Library.
- Duncan, C., Willson, R., Kendall, J., Harrison, R. & Hickey, J. 1982. Latest rocket measurements of the solar constant. *Solar Energy*, 28(5): 385–387.
- Einstein, A. 1911. A new determination of the molecular dimensions (vol 19, pg 289, 1906). *Annalen der physik*, 34(3): 591–592.
- Fröhlich, C. 1977. Contemporary measures of the solar constant. In *The Solar Output and its Variation*. 93.

- Gueymard, C.A. 2018. A reevaluation of the solar constant based on a 42-year total solar irradiance time series and a reconciliation of spaceborne observations. *Solar Energy*, 168: 2–9.
- Hammerschmidt, U. & Sabuga, W. 2000. Transient hot wire (THW) method: uncertainty assessment. *International Journal of Thermophysics*, 21(6): 1255–1278.
- Hemmat Esfe, M. 2017. The Investigation of Effects of Temperature and Nanoparticles Volume Fraction on the Viscosity of Copper Oxide-ethylene Glycol Nanofluids. *Periodica Polytechnica Chemical Engineering*. <https://pp.bme.hu/ch/article/view/9741> 9 April 2019.
- Hickey, J., Alton, B., Griffin, F., Jacobowitz, H., Pellegrino, P., Maschhoff, R., Smith, E. & Haar, T.V. 1982. Extraterrestrial solar irradiance variability two and one-half years of measurements from Nimbus 7. *Solar Energy*, 29(2): 125–127.
- Holman, Jack.P. 2019. *Heat Transfer*. 10th ed. McGraw-Hill Series.
- Horrocks, J. & McLaughlin, E. 1963. Non-steady-state measurements of the thermal conductivities of liquid polyphenyls. *Proceedings of the Royal Society of London. Series A. Mathematical and Physical Sciences*, 273(1353): 259–274.
- Huminic, A., Huminic, G., Fleaca, C., Dumitrache, F. & Morjan, I. 2015. Thermal conductivity, viscosity and surface tension of nanofluids based on FeC nanoparticles. *Powder Technology*, 284: 78–84.
- Hwang, Y.J., Ahn, Y.C., Shin, H.S., Lee, C.G., Kim, G.T., Park, H.S. & Lee, J.K. 2006. Investigation on characteristics of thermal conductivity enhancement of nanofluids. *Current Applied Physics*, 6(6): 1068–1071.
- Kumar, V., Tiwari, A.K. & Ghosh, S.K. 2015. Application of nanofluids in plate heat exchanger: A review. *Energy Conversion and Management*, 105: 1017–1036.
- Li, H., Ha, C.-S. & Kim, I. 2009. Fabrication of Carbon Nanotube/SiO₂ and Carbon Nanotube/SiO₂/Ag Nanoparticles Hybrids by Using Plasma Treatment. *Nanoscale Research Letters*, 4(11): 1384–1388.
- Maiga, S.E.B., Nguyen, C.T., Galanis, N. & Roy, G. 2004. Heat transfer behaviours of nanofluids in a uniformly heated tube. *Superlattices and Microstructures*, 35(3–6): 543–557.

- Maxwell, J.C. 1873. *A treatise on electricity and magnetism*. Oxford: Clarendon Press.
- Mihiretie, B.M., Cederkrantz, D., Rosén, A., Otterberg, H., Sundin, M., Gustafsson, S.E. & Karlsteen, M. 2017. Finite element modeling of the Hot Disc method. *International Journal of Heat and Mass Transfer*, 115: 216–223.
- Mintsa, H.A., Roy, G., Nguyen, C.T. & Doucet, D. 2009. New temperature dependent thermal conductivity data for water-based nanofluids. *International Journal of Thermal Sciences*, 48(2): 363–371.
- Pramuanjaroenkij, A., Tongkratoke, A. & Kakaç, S. 2018. Numerical Study of Mixing Thermal Conductivity Models for Nanofluid Heat Transfer Enhancement. *Journal of Engineering Physics and Thermophysics*, 91(1): 104–114.
- Sarbu, I. & Sebarchievici, C. 2017. Solar Collectors. In *Solar Heating and Cooling Systems*. Elsevier: 29–97.
<https://linkinghub.elsevier.com/retrieve/pii/B9780128116623000037> 25 April 2019.
- Shima, P.D. & Philip, J. 2014. Role of Thermal Conductivity of Dispersed Nanoparticles on Heat Transfer Properties of Nanofluid. *Industrial & Engineering Chemistry Research*, 53(2): 980–988.
- Singh, K. 2014. Solar Water Heater with Parabolic Concentrator & Preheated Water Inlet. , 1(6): 4.
- Sözen, A., Menlik, T. & Ünvar, S. 2008. Determination of efficiency of flat-plate solar collectors using neural network approach. *Expert Systems with Applications*, 35(4): 1533–1539.
- Spencer, J. 1971. Fourier series representation of the position of the sun. *Search*, 2(5): 172–172.
- Stine, W.B. & Geyer, M. 2001. *Power from the Sun*. Power from the sun. net.
- Struckmann, F. 2008. Analysis of a Flat-plate Solar Collector. : 4.
- Suresh, S., Venkataraj, K.P., Selvakumar, P. & Chandrasekar, M. 2012. Effect of Al₂O₃-Cu/water hybrid nanofluid in heat transfer. *Experimental Thermal and Fluid Science*, 38: 54–60.
- Teng, T.-P., Hung, Y.-H., Teng, T.-C., Mo, H.-E. & Hsu, H.-G. 2010. The effect of alumina/water nanofluid particle size on thermal conductivity. *Applied Thermal Engineering*, 30(14–15): 2213–2218.

- Wang, X., Xu, X. & S. Choi, S.U. 1999. Thermal Conductivity of Nanoparticle - Fluid Mixture. *Journal of Thermophysics and Heat Transfer*, 13(4): 474–480.
- Wilson, B. 1962. The role of solar energy in the drying of vine fruit. *Australian Journal of Agricultural Research*, 13(4): 662–673.
- Xie, H., Wang, J., Xi, T. & Liu, Y. 2002. Thermal conductivity of suspensions containing nanosized SiC particles. *International Journal of Thermophysics*, 23(2): 571–580.
- Xuan, Y. & Roetzel, W. 2000. Conceptions for heat transfer correlation of nanofuids. *Int. J. Heat Mass Transfer*: 7.
- Yu, W. & Choi, S.U.S. 2003. The Role of Interfacial Layers in the Enhanced Thermal Conductivity of Nanofluids: A Renovated Maxwell Model. *Journal of Nanoparticle Research*, 5(1/2): 167–171.
- Yurddaş, A. 2013. *Nanoakışkanlı Düzlemsel Güneş Kollektörlerinde Isı transferi Analizi*. Msc. Thesis. Manisa: Celal Bayar Üniversitesi.
- Zhu, H., Lin, Y. & Yin, Y. 2004. A novel one-step chemical method for preparation of copper nanofluids. *Journal of Colloid and Interface Science*, 277(1): 100–103.

APPENDIXES

Appendix 1. Function Library for Top Heat Loss Coefficient Calculation

```

"""Function Library for Top Heat Loss Coefficient
Calculation"""

# -*- coding: utf-8 -*-
"""
Created on Tue Nov 13 07:34:30 2018
@author: zafer.aksoz
"""

#Reuired Packages
from math import cos,sin

#Average air temperature between absorber plate and glass
def Tair(T_p,T_g):
    return ((T_p+T_g)/2)

#Temperature difference between absorber plate and glass
def deltaT(T_p,T_g):
    return (T_p-T_g)

#Temperature of air between absorber and glass
def Tairkelvin(T_air):
    return (T_air+273)

#Rayleigh Number
def ray(g,delta_T,L,v,Pr, T_air_kelvin):
    return ((g * delta_T * (L**3) * Pr)/(T_air_kelvin *
(v**2)))

#Converting temperatures from Celcius to Kelvin
def Tgk(T_g):
    return (T_g+273)

#Absorber Plate Temperature
def Tpk(T_p):
    return (T_p+273)

#Sky and Abient Temperature
def Tsk(T_s):
    return (T_s+273)

```

```

#The radiative heat transfer coefficient from the cover to
the sky
def hrs(epsilon_g,sigma,T_g_k,T_s_k):
    return
    (epsilon_g*sigma*(T_g_k+T_s_k)*((T_g_k**2)+(T_s_k**2)))

#The radiative heat transfer coefficient from plate to cover
def hrg(sigma,T_p_k,T_g_k,epsilon_p,epsilon_g):
    return
    (((sigma)*((T_p_k**2)+(T_g_k**2))*(T_p_k+T_g_k))*(((1/epsilon_p)+
    (1/epsilon_g))-1)**(-1))

#Nusselt Number
def Nuss(Ra,beta):
    return (1+((1.44)*(1-(1708/(Ra*cos(beta))))*(1-
    ((1708*sin((1.8*beta)**(1.6)))/(Ra*cos(beta)))))+(((Ra*cos(
    beta))/(5830))**(1/3))-1))

#The convective heat transfer coefficient between the plate
and cover
def hcp(Nu,k,L):
    return ((Nu*k)/L)

#Top heat loss coefficient
def Ut(h_cp,h_w,h_rg,h_rs):
    return (((1/(h_cp+h_rg))+1/(h_w+h_rs))**(-1))

#Glass Temperature
def Tg(T_p, U_t, T_s,h_cp,h_rg):
    return (T_p-(((U_t)*(T_p-T_s))/(h_cp+h_rg)))

#####

```

Appendix 2. Collector Top Heat Loss Coefficient

```

"""Collector Top Heat Loss Coefficient"""

import HeatLossLibrary2 as hl
import numpy as np
from scipy import interpolate
from math import cos,sin
from numpy import genfromtxt
import os
import matplotlib.pyplot as pl

#Guess value of glass temperature
T_g=30

#Glazing Space(plate-to-cover space)
L=0.025

#Specific Gravity
g=9.81

#Collector Tilt angle
beta=45

#Glass emissivity
epsilon_g=0.88

#Absorber plate emissivity
epsilon_p=0.95

#Stephan-Boltzman Constant
sigma=5.67E-08

#Sky or ambient temperature
T_s=20

#Convective heat loss coefficient of the wind
h_w=10

#Table Data#

data = genfromtxt(r'C:\Users\zafer.aksoz\Desktop\MY OWN
STUDY\tm.csv', delimiter=',')

```

```

#temperature of air from table
temp = data[:,0]

#density
density=data[:,1]
#thermal conductivity of air
cond=data[:,2]

#kinematic viscosiy
vis=data[:,5]

#prandtl number
Pra=data[:,6]

#Functions for Linear Interpolation from data

f_rho=interpolate.interp1d(temp,density)
f_k=interpolate.interp1d(temp,cond)
f_vis=interpolate.interp1d(temp,vis)
f_Pra=interpolate.interp1d(temp,Pra)
##
#Galss Emissivity
Eps=0.01

UT=[]
Tp=[]

for T_p in range(30,100,1):

    print("T_p:", T_p)

    while True:

        T_air = hl.Tair(T_p,T_g)

        #making interpolation

        #Density of the air
        rho = f_rho(T_air)
        #Thermal Conductivity of air

```

```

k = f_k(T_air)
#Dynamic viscosity of air
v = f_vis(T_air)
#Prandtl Number
Pr = f_Pra(T_air)
#Temperature difference between glass and plate
delta_T=hl.deltaT(T_p,T_g)
#Air as Kelvin Unit
T_air_kelvin=hl.Tairkelvin(T_air)
#Rayleigh Number
Ra=hl.ray(g,delta_T,L,v,Pr, T_air_kelvin)
#Nusselt Number
Nu=hl.Nuss(Ra,beta)
#Glass Temperature as Kelvin
T_g_k=hl.Tgk(T_g)
#Plate Temperature as Kelvin
T_p_k=hl.Tpk(T_p)
#Sky Temperature [K]
T_s_k=hl.Tsk(T_s)
#Convective heat transfer coefficient
h_cp=hl.hcp(Nu,k,L)
#The radiation coefficient from plate to
cover(glass)
h_rg=hl.hrg(sigma,T_p_k,T_g_k,epsilon_p,epsilon_g)
#The radiation coefficient from cover to sky
h_rs=hl.hrs(epsilon_g,sigma,T_g_k,T_s_k)

#Top heat loss coefficient
U_t=hl.Ut(h_cp,h_w,h_rg,h_rs)

#
T_g_new = hl.Tg(T_p, U_t, T_s,h_cp,h_rg)

print ("T_air:",T_air)
print ("rho:", rho)
print ("k:", k)
print ("v:", '{:.20f}'.format(v))
print ("Pr:", Pr)
print ("delta_T:", delta_T)
print ("T_air_kelvin:", T_air_kelvin)
print ("Ra:", Ra )
print ("Nu:", Nu)
print ("h_cp:", h_cp)
print ("T_p_k:", T_p_k)
print ("T_g_k:", T_g_k)

```

```

print ("T_s_k:", T_s_k)
print ("h_rg:", h_rg)
print ("h_rs:", h_rs)
print ("U_t:", U_t)
print ('T_g_new: ', T_g_new, end=' / ')
print ('T_g_old: ', T_g, end='\n')

if np.abs(T_g -T_g_new) < 0.0001:
    print("T_g_new:", T_g_new)
    break
T_g = T_g_new

```

```

print("T_p:", T_p)
Tp.append(T_p)
UT.append(U_t)

```

```

d_Tp='C:\\Users\\zafer.aksoz\\Desktop\\Tp4.csv'
np.savetxt(d_Tp, Tp)
##
d_TU='C:\\Users\\zafer.aksoz\\Desktop\\TU4.csv'
np.savetxt(d_TU, UT)
pl.ylabel('Top Heat Loss Coefficient  $$(U_L)$(W/m^2K)$')
pl.xlabel('Absorber Plate Temperature  $$(^{\circ}C)$')
pl.plot(Tp[1:],UT[1:], 'b')
pl.show()
#####$$ 
```

Appendix 3. Function Library for Convection heat transfer Coefficient

```

"""Function Library for Convection heat transfer
Coefficient"""

#Pi Number
pi=3.141593

def f_A_s(Pi,D):
    return((pi*(D**2))/(4))

def f_V_avg(m,rho,A_s):
    return((m)/(rho*A_s))

def f_Re(rho,V_avg,D,mu):
    return((rho*V_avg*D)/(mu))

def f_Nu(D,L,Re,Pr):
    return((3.66)+(((0.065*(D/L)*Re*Pr))/((1)+(0.04*(D/L)*
Re*Pr)**(2/3))))

def f_h(Nu,k,D):
    return((Nu*k)/(D))

#####
#####

```


Appendix 4. Heat Transfer Coefficient of the 1% Al₂O₃ Nanofluid

```

"""Heat Transfer Coefficient of the 1% Al2O3 Working
Fluid"""

# Importing the fuction library

import hcal as h
import matplotlib.pyplot as plt
from math import cos,sin

#Required paramaters and their values

#Pi number
pi=3.141593

#Tube diameter
D=0.01

#Mass flow rate
m=0.02

#Length of the pipe
L=10

#obtained data from nanofluid property table
rho=1027.5022

#Dynamic Viscosity
mu=0.0010021

#Thermal Conductivity
k=0.62226

#Prandtl Number
Pr=6.358673092

#Surface area of the pipe through which liquid is carried
away
A_s=h.f_A_s(pi,D)

#Average velocity of the fluid
V_avg=h.f_V_avg(m,rho,A_s)

```

```
#Reynolds number
Re=h.f_Re(rho,V_avg,D,mu)

#Proper Nusselt Number for the flow type i.e. laminar
Nu=h.f_Nu(D,L,Re,Pr)

#Heat transfer coefficient of the working fluid
h_inf=h.f_h(Nu,k,D)

#Printing Values

print("A_s:", A_s)
print("V_avg:", V_avg)
print("Re:", Re)
print("Nu:", Nu)
print("h_inf:", h_inf)
#####
```

Appendix 5. Function Library for Collector Efficiency Calculation

```

"""Function Library for Collector Efficiency Calculation"""

import math

#Average Transmittance-Absorptance Product
def f_Tau_alpha_ave(Tau,Alpha):
    return(0.96*Tau*Alpha)

#Absorbed Solar Radiation
def f_S(Tau_alpha_ave,I_t):
    return(Tau_alpha_ave*I_t)

#Bottom heat loss coefficient
def f_U_b(k_b,L_b):
    return(k_b/L_b)

#Overall heat loss coefficient
def f_U_L(U_t,U_b,U_e):
    return(U_t+U_b+U_e)

#m value in fin equation
def f_m_fin(U_L,k_p,delta_p):
    return(math.sqrt((U_L)/(k_p*delta_p)))

#Total heat loss coefficient
def f_U_L(U_t,U_b,U_e):
    return(U_t+U_b+U_e)

#Fin efficiency
def f_F_fin(m_fin,W,D):
    return((math.tanh((m_fin)*((W-D)/2)))/(((m_fin)*((W-D)/2))))

#collector efficiency factor
def f_f_prime(U_L,D,W,F_fin,pi,D_i,h_fi):
    ust = 1/U_L
    p_ilk = 1/(U_L*(D+(W-D)*F_fin))
    p_iki = 1/(math.pi*D_i*h_fi)
    return ust/(W*(p_ilk+p_iki))

```

#Heat removal factor

```
def f_F_R(m,C_p,A_c,U_L,F_prime):
    R=((m*C_p)/(A_c*U_L))
    return(R*(1-math.exp((-1)*((1/R)*F_prime))))
```

#Useful heat gain by the collector

```
def f_Qu(F_R,Tau,Alpha,T_f_i,T_a,U_L,A_c,G_t):
    return((F_R*(Tau*Alpha)*A_c*G_t)-(((F_R*U_L)*(T_f_i-
T_a))))
```

#Overall thermal efficiency of the flat-plate solar collector

```
def f_eta(Qu,A_c,G_T):
    return((Qu/(A_c*G_T)))
```

=====

#Reduced Temperature Parameter

```
def f_redtemp(T_f_i,T_a,G_t):
    return((T_f_i-T_a)/G_t)
```

#Collector outlet temperature

```
def f_T_f_o(T_f_i,Qu,m,C_p):
    return(T_f_i+((Qu)/(m*C_p)))
```

#Maximum Useful Heat Gain by the working fluid

```
def f_Q_u_2(m,C_p,T_f_i,T_f_o):
    return(m*C_p*(T_f_o-T_f_i))
```

#####

Appendix 6. Flat-plate Solar Collector Efficiency Calculation

```
""" Efficiency Calculations for 1% Al2O3 Nanofluid """
```

```
import funlib2 as eff
import numpy as np
import matplotlib.pyplot as plt
import math

#Creating arrays for parameters
FR_arr=[]
redtemp_arr=[]
eta_arr=[]
Tfi_arr=[]
Tfo_arr=[]
Qu_arr=[]
Qu2_arr=[]

#Initial working fluid inlet temperature
T_f_i=20

while True:

    #Pi number
    pi=3.141593

    #fluid inlet temperature
    Tfi_arr.append(T_f_i)

    #Collector area
    A_c=1

    #Tube Spacing(Distance between tubes)
    W=0.15

    #Tube Diameter
    D=0.01

    #Fluid inlet diameter
    D_i=0.01
```

```
#Transmittance
Tau=0.94

#Absorptance
Alpha=1

#Ambient temperature
T_a=20

#Solar Radiation
G_t=800

#Density of the fluid
rho=1146.391

#heat capacity of the fluid
C_p=3948.45616

#heat transfer coefficient of the inlet fluid
h_fi=290.0109462

#Mass flow rate
m=0.02
U_L=7.4
F_fin=0.9416078

#collector efficiency factor
F_prime=eff.f_f_prime(U_L,D,W,F_fin,pi,D_i,h_fi)
print("F_prime:", F_prime)

Z=eff.f_Z(m,C_p,A_c,U_L,F_prime)
print("Z:",Z)

#collector flow factor
F_double_prime=eff.f_double_prime(Z)
print("F'':", F_double_prime)

#Heat removal factor
F_R=eff.f_F_R(F_prime,F_double_prime)
FR_arr.append(F_R)
```

```

print("F_R;",F_R )

#Maximum possible useful heat gain
Qu=eff.f_Qu(F_R,Tau,Alpha,T_f_i,T_a,U_L,A_c,G_t)
Qu_arr.append(Qu)
print("Qu;",Qu)

#Overall Instantaneous thermal efficiency of the FPSC
eta=eff.f_eta(Qu,A_c,G_t)
eta_arr.append(eta)
print("efficiency:", eta)

#Reduced Temperature Parameter
redtemp=eff.f_redtemp(T_f_i,T_a,G_t)
redtemp_arr.append(redtemp)
print("redtemp:", redtemp)

#Working fluid inlet temperature
print("T_f_i:", T_f_i)

#Working fluid outlet temperature
T_f_o=eff.f_T_f_o(T_f_i,Qu,m,C_p)
Tfo_arr.append(T_f_o)
print("T_f_o:", T_f_o)

#Maximum Useful Heat Gain by the working fluid
#(Working fluid inlet and outlet temperatures, mass
#flow rate and heat capacity of the fluid were taken
into consideration)

Q_u_2=eff.f_Q_u_2(m,C_p,T_f_i,T_f_o)
Qu2_arr.append(Q_u_2)
print("Q_u_2:", Q_u_2)

T_f_i=T_f_o

if T_f_i>80:
    break
#Loop ends
#####
#Data Saving

```

```
#####
```

```
d_F_R='C:\\Users\\zafer.aksoz\\Desktop\\DAT2\\FR1.csv'
np.savetxt(d_F_R,FR_arr)
```

```
d_redtemp='C:\\Users\\zafer.aksoz\\Desktop\\DAT2\\REDTEMP1.csv'
```

```
np.savetxt(d_redtemp,redtemp_arr)
```

```
#
```

```
d_eta='C:\\Users\\zafer.aksoz\\Desktop\\DAT2\\EFFICIENCY1.csv'
```

```
np.savetxt(d_eta,eta_arr)
```

```
d_Tfi='C:\\Users\\zafer.aksoz\\Desktop\\DAT2\\TFI1.csv'
```

```
np.savetxt(d_Tfi,Tfi_arr)
```

```
#
```

```
d_Tfo='C:\\Users\\zafer.aksoz\\Desktop\\DAT2\\TF01.csv'
```

```
np.savetxt(d_Tfo,Tfo_arr)
```

```
#
```

```
d_Qu='C:\\Users\\zafer.aksoz\\Desktop\\DAT2\\QU1-1.csv'
```

```
np.savetxt(d_Qu,Qu_arr)
```

```
d_Qu_2='C:\\Users\\zafer.aksoz\\Desktop\\DAT2\\QU2-1.csv'
```

```
np.savetxt(d_Qu_2,Qu2_arr)
```

```
#####
```

```
"""Plotting Data"""
```

```
v1=redtemp_arr
```

```
v2=eta_arr
```

```
plt.xlabel("Reduced temperature parameter [ $^{\circ}\text{Cm}^2/\text{W}$ ])")
```

```
plt.ylabel("Efficiency"+ r'($\eta_i$)')
```

```
plt.plot(v1,v2,'k')
```

```
plt.legend(('Efficiency'),loc=0)
```

```
plt.show()
```


RESUME

PERSONEL INFORMATION

Name Surname : Zafer Yavuz AKSÖZ

Place and Date Of Birth : 25.09.1992

Education

Undergraduate : Energy Systems Engineering/SDU

Post Graduate : Mechanical Engineering/ADU

Foreign Languages : English

Scientific Activities

A) Proceedings

Contact

E-mail : zafer.aksoz@bilgi.edu.tr

Date :11/06/2019